WILEY-BLACKWELL

Cladistics 36 (2020) 301–321

Cladistics

10.1111/cla.12407

A species-level total evidence phylogeny of the microteiid lizard family Alopoglossidae (Squamata: Gymnophthalmoidea)

Cristian Hernández Morales[a,b,c]*, Marcelo J. Sturaro[a,d], Pedro M. Sales Nunes[e], Sebastian Lotzkat[f] and Pedro L.V. Peloso[c]

[a]*Museu Paraense Emílio Goeldi, Coordenação de Zoologia, Avenida Perimetral, 1901, Terra-Firme, CEP 66077-530, Belém, Pará, Brazil;* [b]*Department of Biological Sciences, Sam Houston State University, 1900 Avenue I, Huntsville, TX, 77341, USA;* [c]*Instituto de Ciências Biológicas, Universidade Federal do Pará, Rua Augusto Corrêa, 01, Guamá, CEP 66075-110, Belém, Pará, Brazil;* [d]*Departamento de Ecologia e Biologia Evolutiva, Universidade Federal de São Paulo, Av. Professor Artur Riedel, 275, Jardim Eldorado, CEP 09972-270, Diadema, São Paulo, Brazil;* [e]*Universidade Federal de Pernambuco, Av. Professor Moraes Rego s/n, Cidade Universitária, 50670-901, Recife, Pernambuco, Brazil;* [f]*Staatliches Museum für Naturkunde Stuttgart, Rosenstein 1, 70191, Stuttgart, Germany*

Accepted 22 October 2019

Abstract

Alopoglossidae is a family of Neotropical lizards composed of 23 species allocated in two genera (*Alopoglossus* and *Ptychoglossus*). There is a lack of knowledge about the phylogenetic relationships and systematics of this family. Published phylogenies that include alopoglossid species have very low taxon coverage within the family, and are usually based on limited character sampling. Considering these shortcomings, we infer the phylogenetic relationships of Alopoglossidae—including all but one species in the family—based on the combined analyses of DNA sequences and morphological characters. We use four loci (the mitochondrial *12S*, *16S* and *ND4*; the nuclear C-mos) and a matrix of 143 phenotypic characters from scutellation, tongue morphology, hemipenis morphology, and osteology. The dataset is analyzed with Maximum Parsimony, with four alternative weighting schemes: three under Extended Implied Weighting, and one with equal weighting. The respective resulting topologies are compared in a sensitivity analysis framework. Our analyses support the paraphyly of *Ptychoglossus*, with *Alopoglossus* nested within it. We provide an updated classification for the family, where *Ptychoglossus* Boulenger, 1890 is considered a junior synonym of *Alopoglossus* Boulenger, 1885.

Introduction

Alopoglossid lizards are distributed from Costa Rica through northern South America, both east and west of the Andes, and across Amazonia (Harris, 1994; Köhler et al., 2012; Uetz and Hallerman, 2014). These are diurnal miniaturized lizards that inhabit the leaf litter of Neotropical forests and crops, where their brownish coloration and cryptic behavior help them to blend in with the environment (Anaya-Rojas et al., 2010; Bolívar-G and Hernandez-Morales, 2013; Meza-Joya et al., 2014).

Alopoglossidae, as currently defined, is composed of two genera: *Alopoglossus* Boulenger, 1885 (nine valid nominal species) and *Ptychoglossus* Boulenger, 1890 (14 valid nominal species). The family was, for a long time, recognized as a sub-family of Gymnophthalmidae (Pellegrino et al., 2001; Castoe et al., 2004; Pyron et al., 2013), but recently separated from the latter and elevated to full family status by Goicoechea et al. (2016)—based on the results of phylogenetic analyses of DNA sequence data. Goicoechea et al. (2016) performed several analyses on their dataset, but based their taxonomic decision on a preferred phylogenetic hypothesis—i.e., derived from a parsimony analysis and the direct optimization (*sensu* Wheeler, 1996) of nucleotide sequence characters. Based on that hypothesis, Alopoglossidae

*Corresponding author:
E-mail address: nandezsendo@gmail.com

was recovered as the sister clade of Teiidae + Gymnophthalmidae, and thus recognized as a separate family. Whether Alopoglossidae is the sister group of Gymnophthalmidae or of Teiidae + Gymnophthalmidae is still somewhat controversial, but the monophyly of Alopoglossidae has been consistently supported by both morphological (Presch, 1980) and molecular data (Castoe et al., 2004; Pyron et al., 2013). Nevertheless, to date, there are no published phylogenetic analyses that include the majority of the valid species of Alopoglossidae, and phylogenetic analyses of Gymnophthalmoidea that incorporate both phenotypic and genomic data simultaneously are very limited.

The most comprehensive study on alopoglossid phylogeny was an exclusively molecular-based study, which relied on a single mitochondrial gene (ND4)—the study was, however, limited to *Alopoglossus* (Torres-Carvajal and Lobos, 2014). Their dataset included most recognized species of *Alopoglossus* (except *A. lehmanni* Ayala and Harris, 1984, known only from the holotype, and the recently named *A. embera* Peloso and Hernandez-Morales, 2017, and *A. meloi* Ribeiro-Júnior, 2018). A single species of *Ptychoglossus* was included, to root the tree, thereby assuming the monophyly of *Alopoglossus*. On the other hand, for *Ptychoglossus*, only *P. bre-vifrontalis* Boulenger, 1912 was ever used in any published genomic analysis (Pellegrino et al., 2001; Castoe et al., 2004; Colli et al., 2015; Goicoechea et al., 2016). Biogeographically, Torres-Carvajal and Lobos (2014) reported that the Andes split *Alopogloglossus* in two clades, one Cis-Andean and another Trans-Andean. The geographic distribution of *Ptychoglossus* has never been related to its phylogenetic relationships.

Two phylogenetic studies based strictly on morphological characters included alopoglossid species. Presch (1980) included four alopoglossid species and coded 26 characters (24 osteological and two myological). Hoyos (1998) performed a phylogenetic analysis of some Colombian gymnophthalmid species that included *P. stenolepis* (Boulenger, 1908) using 15 characters, nine osteological and six myological. A few additional studies combined morphological and genotypic data which included at least two alopoglossids—using up to 77 morphological characters and 2333 base pairs of molecular data (Rodrigues et al., 2005, 2007, 2009; Peloso et al., 2011). Although all of these studies included very limited taxonomic sampling of alopoglossids and help little in understanding the relationships among these taxa, they support the sister taxon relationship between the two genera.

As detailed above, the phylogenetic relationships of species within both *Alopoglossus* and *Ptychoglossus* are very poorly understood. There are no available studies specifically designed to test the phylogenetic relationships of *Ptychoglossus*, and the phylogeny available for *Alopoglossus* does not include all of the valid species. With the aim of testing both the monophyly of Alopoglossidae and that of groups within this family, we carried out a phylogenetic study including most recognized alopoglossid species (except *A. meloi* Ribeiro-Junior, 2018) and a comprehensive character sampling comprising both genomic and phenomic evidence. With the phylogeny in hand, we are able to describe the morphological synapomorphies that support the different clades within the tree of Alopoglossidae.

Materials and methods

Our objective to include all known taxa of Alopoglossidae in the phylogeny was met with significant challenges. The most important limitation of our study is the lack of complete character sampling for several ingroup taxa. Three alopoglossid species (*A. lehmanni*, *P. eurylepis* Harris and Rueda, 1985, and *P. grandisquamatus* Rueda, 1985) are known from single specimens, and many other species are represented only by a handful of specimens collected decades ago (Harris, 1994; Peloso and Hernandez-Morales, 2017). This had significant repercussions for the completeness of the dataset. For the genomic partition, we were unable to obtain tissue samples for several species, especially within *Ptychoglossus*. The anatomical character partitions were also affected, as several internal morphological characters could not be sampled due to our inability to dissect or scan specimens of species underrepresented in collections. Moreover, we failed to include *A. meloi*, a recently named species from the Amazonia of Brazil. The species was named after we had completed all of the data collection and analyses. From the original description, *A. meloi* seems to be most similar to *A. angulatus* (Linnaeus, 1758)—we infer a close relationship between the two species.

Taxon sampling

Most currently valid species of Alopoglossidae were included in this study, except *A. meloi*. Outgroup taxa were selected following three requirements: (i) the availability of sequences of the target genes in GenBank (Benson et al., 2013), (ii) prompt availability of specimens that allowed for a complete sampling for the phenotypic characters, (iii) to include a broad representation of taxa closely related to Alopoglossidae (i.e., Gymnophthalmidae and Teiidae). For gymnophthalmids, the following subfamilies were represented in our dataset: Cercosaurinae (*Arthrosaura kockii* (van Lidth de Jeude, 1904); *Bachia flavescens* (Bonnaterre, 1789); *Cercosaura ocellata* Wagler, 1830; *Loxopholis guianense* (Ruibal, 1952); *Potamites ecpleopus* (Cope, 1875)) and Gymnophthalminae (*Colobosaura modesta*

(Reinhardt and Lütken, 1862); *Iphisa elegans* Gray, 1851; *Tretioscincus agilis* (Ruthven, 1916)). For Teiidae, two of the three subfamilies were represented: Teiinae (*Ameiva ameiva* (Linnaeus, 1758); *Cnemidophorus lemniscatus* (Linnaeus, 1758); *Kentropyx calcarata* Spix, 1825) and Tupinambinae (*Tupinambis teguixin* (Linnaeus, 1758) and *Salvator merianae* (Duméril and Bribon, 1839)). The tree was rooted with *Lacerta viridis* (Laurenti, 1768), based on the fact that Lacertidae is consistently recovered as the sister taxon of Gymnophthalmoidea (Conrad, 2008; Gauthier et al., 2012; Pyron et al., 2013; Reeder et al., 2015). The complete list of specimens examined is given in Appendix S1. The complete taxon sampling showing which species had information for each partition of data is included in Appendix S2.

Genotypic evidence

Laboratory protocols. We extracted and isolated genomic DNA from frozen and ethanol-preserved tissues (usually liver or muscle) using the Qiagen DNeasy kit, following the manufacturer's guidelines. We targeted for PCR amplification and sequencing the nuclear DNA (nDNA) gene *Oocyte Maturation Factor Gene* (C-mos), and the mitochondrial DNA (mtDNA) loci *NADH Dehydrogenase Subunit IV* (ND4), and mitochondrial *rRNA subunits 12S* (12S) and *16S* (16S). The primers used for PCR amplification and sequencing have largely been used in lizard phylogenetic studies before, including Alopoglossidae (Kocher et al., 1989; Arevalo et al., 1994; Saint et al., 1998; Pellegrino et al., 2001)—PCR primers and conditions are listed in Table 1. PCR products were sequenced in both directions, using an ABI automated sequencer, and the sequences were assembled, checked for quality and edited in Geneious R9 (Kearse et al., 2012).

Genotypic sampling. We had access to tissue samples from three *Alopoglossus* and seven *Ptychoglossus* species, i.e. 50% of the described diversity within Alopoglossidae. Our data were complemented with sequences of 16S and ND4 of *A. buckleyi* (O'Shaughnessy, 1881), *A. festae* (Peracca, 1896), and *A. viridiceps* Torres-Carvajal and Lobos, 2014, deposited by Torres-Carvajal and Lobos (2014) and Arteaga et al. (2016) in GenBank (Benson et al., 2013). Therefore, 13 of 22 ingroup species have genotypic evidence available. See Appendix S2 for an overview of the genotypic sampling and GenBank accession numbers of newly generated sequences.

Morphological evidence

We designed the morphological dataset to accommodate the variation within Alopoglossidae, but also accounted for variation within the whole Gymnophthalmoidea. We used the program Mesquite, version 3.4 (Maddison and Maddison, 2010) to construct the morphological character sets. We coded a total of 143 morphological characters that can be grouped into seven different partitions, depending on the sources of information, as follows: five characters from tongue morphology, 68 from scutellation, ten from hemipenis, 39 from cranium, five from mandible, eight from postcranial osteology, and eight from the hyoid apparatus. The complete list of characters, including a brief description and delimitation of putatively homologous character states, is provided in Appendix 1 (MorphoBank project number 3351).

Tongue characters were largely based on the morphological studies of Boulenger (1885) and Harris (1985), and we scored these characters in specimens preserved with the mouth opened—in rare cases. When permitted, the tongue was extracted and analyzed separately. For *A. viridiceps*, *P. kugleri* (Roux, 1927), and *P. romaleos* Harris, 1994, we did not have access to tongue morphology. The scutellation was coded following the nomenclature proposed by Harris (1994). Hemipenial characters were coded from the direct observation of the organ. We used some of the hemipenial characters and terminology defined by P. M. S. Nunes (unpublished data). For some species where material was not immediately available, we prepared hemipenes following the protocols of Pesantes (1994) and Zaher and Prudente (2003).

Two techniques were used to code characters related to the osteological partition. For some specimens, we used high-resolution computed tomography scan (CT) scans whereas for others we used cleared and double-stained specimens. We obtained CT scans of *A. angulatus*, *A. buckleyi*, *A. embera*, 2017, *A. festae*, *A. lehmanni*, *P. danieli* Harris, 1994, *P. plicatus* (Taylor, 1949), and *P. vallensis* (Harris, 1994) using GE Phoenix Vtome Xs Micro Computed Tomography machines. The scans were done at the Microscopy and Image Facility (MIF) at the American Museum of Natural History and the Nanoscale Research Facility at the University of Florida. Compilation of the individual X-rays and image 3D visualizations were done in VGStudio MAX version 2.2 (Volume Graphics, Heidelberg, Germany). TIFF images from 3D rendering were used herein for descriptions and comparisons. The osteology of six taxa (*A. angulatus*; *A. atriventris* Duellman, 1973; *P. bicolor* (Werner, 1916); *P. brevifrontalis*; *P. vallensis*; *P. stenolepis*) was analyzed from cleared and double-stained specimens. For newly prepared specimens, we followed the protocol of Maisano (2008).

Phylogenetic analyses

Nucleotide homology was established automatically for each targeted gene using multiple sequence

Table 1
List of primers and summary of PCR conditions used in this study

Gene	Primer	Primer sequence (5′–3′)	Reference	PCR conditions			
				Denaturation	Annealing	Extension	Cycles
12S	12Sa	CTG GGA TTA GAT ACC CCA CTA	Modified from Kocher et al. (1989)	94 °C (1 : 00)	52 °C (1 : 00)	72 °C (1 : 00)	40
	12Sb	TGA GGA GGG TGA CGG GCG GT	Modified from Kocher et al. (1989)				
16S	16SF	CTG TTT ACC AAA AAC ATM RCC TYT AGC	Pellegrino et al. (2001)	94 °C (1 : 00)	53 °C (1 : 00)	72 °C (1 : 00)	40
	16SR	TAG ATA GAA ACC GAC CTG GAT T	Pellegrino et al (2001)				
ND4	ND4F	CAC CTA TGA CTA CCA AAA GCT CAT GTA GAA GC	Arevalo et al. (1994)	94 °C (1 : 00)	53 °C (1 : 00)	72 °C (1 : 00)	40
	ND4R	CAT TAC TTT TAC TTG GAT TTG CAC CA	Arevalo et al. (1994)				
C-mos	G73	GCG GTA AAG CAG GTG AAG AAA	Saint et al. (1998)	94 °C (1 : 00)	53 °C (1 : 00)	72 °C (1 : 00)	40
	G74	TGA GCA TCC AAA GTC TCC AAT C	Saint et al. (1998)				

alignment (MSA) in MAFFT using the default parameters (Katoh et al., 2005). We performed phylogenetic inference analyses under the parsimony (PAR) optimality criteria, using Extended Implied Weighting (Goloboff, 1993, 2014) and the more widely used equally weighted parsimony—all analyses were performed in TNT (Goloboff et al., 2008). Tree searches were performed with one thousand replicates, with a minimum of ten hits under the *xmult* command, which implements a variety of tree search algorithms—Random Addition Sequences (RAS), Tree Bisection and Reconnection branch swapping (TBR), Parsimony Ratchet (Nixon, 1999), Tree Fusing (Goloboff, 1999), Sectorial Searches (Goloboff, 1999), and Tree Drifting (Goloboff, 1999).

Extended Implied Weighting analysis weights characters, during tree search, according to their level of homoplasy, assigning greater weights to the hierarchic characters and down-weighting homoplastic characters. Given that different sources of characters can have different levels of homoplasy, the data set was divided in four partitions to better accommodate such variation—into a morphological set, an rRNA set where the 12S and 16S markers were concatenated in SequenceMatrix (Vaidaya et al., 2011), and two separate sets for the protein coding loci, ND4 and C-mos, respectively. To assess the effect of the weighting scheme on the topologies, we tested four alternative schemes: (i) Independent Character Weighting—weighting each single character separately; (ii) Collectively Weighted—in the morphological partition each character weighted independently, each ribosomal marker as well as the respective 1st, 2nd, and 3rd positions of each protein coding gene weighted collectively; (iii) Non-Extrapolating Collectively Weighted—same weighting scheme as ii, but without extrapolating the average homoplasy to the missing entries; and (iv) Equally Weighted—unweighted Parsimony.

The Extended Implied Weighting needs a reference constant value (k), whereby the lower the k, the stronger the down-weighting on the homoplastic characters will be. Finding the optimal k value remains one the most critical steps in Extended Implied Weighting analyses, given that different k values can generate different topologies. We follow Mirande's (2009) strategy —thus, we implemented k values that have an average character fit of 50, 54, 58, 62, 66, 70, 74, 78, 82, 86, and 90% of the fit of a perfectly hierarchic one (see also Reemer and Ståhls, 2013) for each weighting scheme. Table 2 shows the k values calculated for each average character fit percentage, the same values are applied to all the weighting schemes. With this strategy we can avoid the artificially biased impression of stability generated towards higher values when regularly distributed k values are used. This also permits avoidance of overweighting because the stronger k value

Table 2
k values calculated for each average character fit percentage

Average character fit (%)	*k* value
50	1.30
54	1.53
58	1.80
62	2.13
66	2.53
70	3.05
74	3.72
78	4.63
82	5.95
86	8.03
90	11.76
95	24.84

implemented is that in which the "average" character has 50% of the weight of a perfectly hierarchical one. In the case that more than one tree was found for a *k* value, a strict consensus was calculated.

Given that each *k* value may result in different tree topologies—except for the equally weighted scheme where the *k* values are not applied—it is necessary to perform a two-step procedure to choose one tree per weighting scheme and then find an optimal tree (=optimal *k* value) among those trees plus the equally weighted tree. The criteria for choosing among the trees generated with different *k* values for each weighting scheme was nodal stability. Nodal stability was calculated using the SPR distance (Goloboff, 2008), considering as the most stable trees those that have the lowest average differences in relation to the remaining trees. If more than one tree has the same SPR distance, we use the nodal support as a secondary parameter, choosing the tree with the greater value. Nodal support was measured with bootstrapping, with 1000 replicates for each *k* value, with the best-supported tree being that with the greater average bootstrap support. Once the optimal tree had been found for each scheme, the same procedure based on stability and support was implemented to choose among these and the equally weighted tree. The validity of sensitivity analyses using nodal stability and nodal support as a criterion of selection remains controversial (Wheeler, 1995; Giribet et al., 2002; Grant and Kluge, 2005; Giribet and Wheeler, 2007). Nonetheless, we agree with the point of view that this type of analysis provides an objective framework to test for robustness of phylogenetic data (see also Giribet et al., 2002; Giribet and Wheeler, 2007).

In addition to the bootstrap support, relative Goodman-Bremer support (Goodman et al., 1982; Bremer, 1988; Goloboff et al., 2003; Grant and Kluge, 2008) values were calculated for the optimal trees of each weighting scheme from 10 000 suboptimal trees up to 100 steps longer than the optimal trees. These relative Goodman-Bremer values were not considered for the selection of the optimal trees of each weighting scheme. The optimal trees of each weighting scheme were compared using the software YBYRÁ (Machado, 2015), which allows for a visual congruence analysis (illustrated through colored square plots) among all trees generated for the study. YBYRÁ generates color-coded boxes to indicate whether synapomorphies are unambiguous (non-homoplastic), or also occur in other clades (homoplastic) and if they are shared by all terminals in a given clade (unique) or are subsequently transformed into one or more different states within that clade (non-unique).

Results

Phylogenetic analyses

In the Independent Character Weighting scheme, the three *k* values belonging to the interval of 58–78% of average character fit (Table 2) share the greatest SPR distance (0.95758), but the $k = 3.72$ was chosen as the optimal for having the greater average nodal support equal to 56.3 (Table 3). In the case of the Collectively Weighted scheme, the three trees generated by the average character fit interval of 74–82% (Table 2) have the highest average SPR distance value (0.95758). The optimal *k* value for this scheme was 5.96 with an average nodal support of 53.0. Last, in the Non-Extrapolating Collectively Weighted scheme the optimal *k* value was 4.64 with an average nodal support of 52.4. In the Non-Extrapolating Collectively Weighted scheme, the three trees with highest average SPR distance value belong to the 70–78% interval of average character fit. See Table 3 for a summary of these parameters and Appendix S3 for an overview of the average SPR distance values and nodal supports of all trees generated for each weighting scheme.

In the second step of our analysis, exploring the stability of the selected weighted and the unweighted trees, we found that the most stable tree was the one generated by the Collectively Weighted scheme that has an average SPR distance of 0.9495 in relation to the other two weighted trees and the unweighted one (Table 4). Although the Independent Character Weighting scheme tree has the greater average nodal support (Table 3), its average SPR distance is the lowest (0.8788). We gave greater importance to stability; hence, the Collectively Weighted tree was preferred over all other alternative topologies.

A visual congruence analysis of the topologies by means of colored square plots, using as a reference the Collectively Weighted tree, is presented in Fig. 1, whereas individual trees from all alternative weighting

Table 3
Résumé of the parameters belonging to the more stable and supported trees among the different k values for each weighting scheme—the first step of our analysis—in the phylogenetic analyses of Alopoglossidae. The parameters of the rejected trees for each weighting scheme are shown in Appendix S3

Scheme	Interval of the more stable trees (%)	Optimal k value	Fit	Average SPR distance	Average nodal support	Total steps
Single character separated	58–78	3.72	376.24065	0.95758	56.3	5458
Weighted collectively	74–82	5.96	382.51760	0.95758	53.0	5454
Non-extrapolating homoplasy	70–78	4.64	471.36637	0.96061	52.4	5454

Table 4
Résumé of the parameters used to choose between the selected trees of each weighting scheme including Equally Weighted–second step of our analysis

Scheme	Average SPR distance	Average nodal support	Total steps
Single character separated	0.8788	56.3	5458
Weighted collectively	0.9495	53.0	5454
Non-extrapolating homoplasy	0.9091	52.4	5454
Equally weighted	0.9394	51.1	5464

schemes are shown separately in Fig. 2. The congruence analysis shows that the Collectively Weighted and the Non-Extrapolating Collectively Weighted schemes generated the same topology, but incongruences appear when these are compared with those produced through the Independent Character Weighting (Fig. 2c) and Equally Weighted (Fig. 2d) schemes. The topology of the Equally Weighted tree is very similar to the preferred scheme. Within the ingroup the two incongruent nodes of the Equally Weighted scheme are not because the members of that node change, but due to the nodes being collapsed (Fig. 2d). In the outgroup, the Equally Weighted and Collectively Weighted trees exhibit incongruences within Gymnophthalmidae. In the Equally Weighted tree, Gymnophthalminae (*C. modesta*, *I. elegans* and *T. agilis*) is the sister group of *B. flavescens*, *C. ocellata* and *P. ecpleopus*, whereas in the case of the Collectively Weighted scheme, it is the sister of *A. kockii* and *L. guianense*. In both cases, Gymnophthalmidae is monophyletic, but both are incongruent with the recently reported relationships of Gymnophthalmidae (Goicoechea et al., 2016). Our outgroup sampling is not inclusive enough for us to propose an update on the widely accepted inner relationships of Gymnophthalmidae—our comments on this topic are only to show the topological variants among the different implemented schemes.

Phylogenetic relationships of Alopoglossidae

In our preferred tree (Fig. 1), generated by the Collectively Weighted scheme, *Alopoglossus* is recovered as monophyletic (albeit nested in a paraphyletic *Ptychoglossus*). *Alopoglossus buckleyi* is sister of *A. atriventris* plus (*A. copii* Boulenger, 1885 and *A. angulatus*), forming the sister clade of *A. embera* plus (*A. festae* and *A. viridiceps*). *Alopoglossus lehmanni* is the sister taxon of all other *Alopoglossus* (Fig. 1). Surprisingly, *Ptychoglossus* is recovered as paraphyletic. *Ptychoglossus bilineatus* (Boulenger, 1890) is the sister taxon of all *Alopoglossus* samples, whereas *P. vallensis* is the sister taxon of *Alopoglossus* plus *P. bilineatus*. The majority of *Ptychoglossus* (*P. bicolor*, *P. brevifrontalis*, *P. eurylepis*, *P. festae* (Peracca, 1896), *P. gorgonae* Harris, 1994, *P. grandisquamatus*, *P. romaleos,* and *P. stenolepis*) form the sister group of this clade including *Alopoglossus*. *Ptychoglossus myersi* Harris, 1994 and *P. plicatus* are grouped in another clade that is sister to the former two. Finally, *P. danieli* and *P. kugleri* form the sister group of all other alopoglossids.

As mentioned above, the Independent Character Weighting scheme was the most divergent (Fig. 2c) from the remaining schemes. In this scheme, *P. kugleri* is recovered as the sister group of Gymnophthalmidae + Alopoglossidae. Moreover, *P. vallensis* and *P. bilineatus* are not closely related to *Alopoglossus*, but cluster with the remaining *Ptychoglossus*. In all schemes, Teiidae is recovered as non-monophyletic.

Discussion

Teiidae were recovered as paraphyletic in all of the analyses, with both Teiinae (*A. ameiva*, *C. lemniscatus,* and *K. calcarata*) and Tupinambinae (*T. teguixin* and *S. merianae*) recovered as monophyletic with high support, respectively. These results differ from previous studies that recovered this family as monophyletic

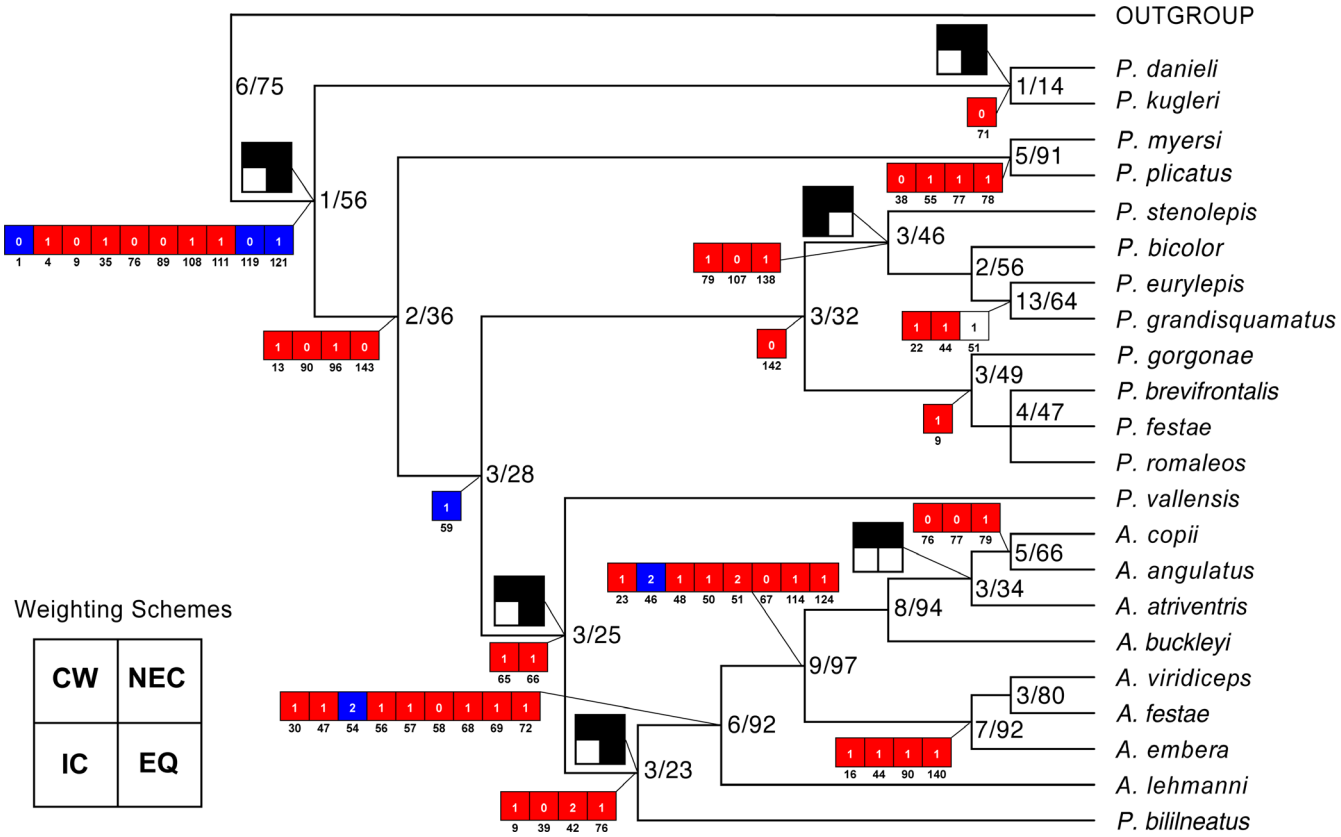

Fig. 1. The phylogenetic relationships within Alopoglossidae, based on molecular and morphological data, shown as the preferred topology (Collectively Weighted scheme). Colored square (black and white) plots indicate incongruence with respect to the alternative weighting schemes: Collectively Weighted—CW, (b) Non-Extrapolating Collectively Weighted—NEC, (c) Independent Character Weighted—IC, and (d) Equally Weighted—EQ. Selected nodes are labeled with derived states (synapomorphies) that support the clade. Character numbers are given below squares, whereas character state numbers are given inside squares. White squares = ambiguous synapomorphies (homoplastic); red squares = non-ambiguous, unique, synapomorphies; blue squares = non-ambiguous, non-unique synapomorphies. Numbers at nodes = relative Goodman-Bremer/bootstrap proportions. This figure is available in color in the online version of the paper. [Colour figure can be viewed at wileyonlinelibrary.com]

(Goicoechea et al., 2016). Our sampling is smaller than that of previous studies and our study was not designed to test the monophyly of Teiidae. We, therefore, refrain from commenting further on the taxonomy of these outgroups beyond a brief note that if these two subfamilies were to be formally recognized as separate families, the names Teiidae Gray, 1827 and Tupinambidae Gray, 1825 are applicable.

The need for an updated taxonomy of Alopoglossidae

Our results corroborate the monophyly of Alopoglossidae, which is supported by at least 10 unambiguous phenotypic synapomorphies (Fig. 1). The analyses also strongly indicate the paraphyly of *Ptychoglossus*. The species currently allocated to this genus are distributed among four different clades, with a monophyletic *Alopoglossus* nested within a clade containing *P. vallensis* and *P. bilineatus* (Fig. 1)—there is, therefore, a necessity of a reappraisal of the taxonomic arrangement in Alopoglossidae. Given the position of *Alopoglossus* with respect to *Ptychoglossus*, few options are available—most of which would result in a complete overhaul of the taxonomy and the creation of several small new genera. We do not favor such drastic changes and, therefore, opted for a simpler solution to the problem. We consider *Ptychoglossus* Boulenger, 1890 as a junior synonym of *Alopoglossus* Boulenger, 1885, and transfer all nominal *Ptychoglossus* species to *Alopoglossus*. We prefer this conservative arrangement instead of, for example, the alternative option of splitting *Ptychoglossus* in multiple genera and transferring *P. bilineatus* and *P. vallensis* to *Alopoglossus*. If we decided to split *Ptychoglossus*, it would be necessary to create at least three new genera inasmuch as the type species of the genus *Ptychoglossus* (*P. bilineatus*) is part of the *Alopoglossus* clade. Hence, the other three clades that contain *Ptychoglossus* species will need new generic names. This option is inconvenient for a series of reasons. Collectively, *Alopoglossus* + *Ptychoglossus* are easily diagnosable, whereas splitting this clade into multiple genera would result in smaller but undiagnosable groups.

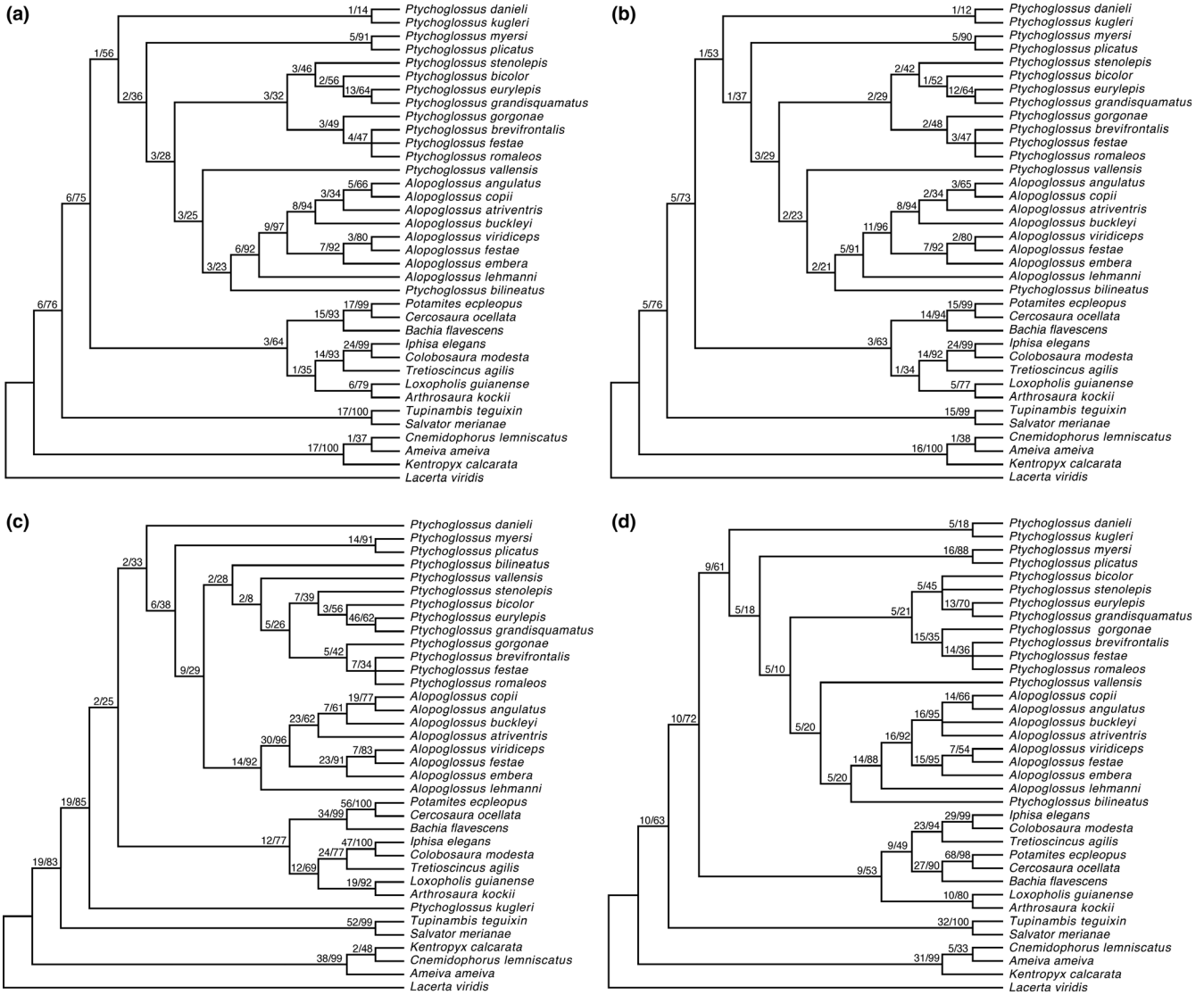

Fig. 2. Selected trees generated by the four weighting schemes: (a) Collectively Weighted—CW, (b) Non-Extrapolating Collectively Weighted—NEC, (c) Independent Character Weighted—IC, and (d) Equally Weighted—EQ. Numbers at nodes = relative Goodman-Bremer/bootstrap proportions.

Our proposed arrangement, however, produces a secondary homonymy between *P. festae* (Peracca, 1896) (senior homonym) and *A. festae* Peracca, 1904 (junior homonym). To solve this, a new name must be given to the junior synonym, and we propose the name *A. harrisi* nom. nov. Etymology—the name is given in honor of Dennis Harris, for his outstanding contributions to the taxonomy of Alopoglossidae. Harris completed the only available review of the genus *Ptychoglossus*, and figures as an author in the descriptions of almost one third of the currently known alopoglossid species (seven out of 23; Ayala and Harris, 1984; Harris and Rueda, 1985; Harris, 1994). In the light of the generic arrangement for the family as proposed herein, below we provide an updated diagnosis for *Alopoglossus,* and thus also for the now monogeneric Alopoglossidae. A summary of the new species-level taxonomy is given in Table 5.

Alopoglossus Boulenger, 1885

Type species: *Alopoglossus angulatus* (Linnaeus, 1758).

Diagnosis

Members of *Alopoglossus* (=Alopoglossidae) can be distinguished from other gymnophthalmoids by: (i) having the tongue entirely covered by oblique plicae (only partially covered by oblique plicae or covered with scale-like papillae in other gymnophthalmoids); (ii) *cristae cranii* of the frontal forming a tubular structure (flanged in *Gymnophthalmus* and *Heterodactylus*); (iii) the presence of postorbitofrontal (also present in

Table 5
Taxonomic updates resulting from the new generic arrangement of Alopoglossidae. *A. meloi* not included in our analyses

Alopoglosus angulatus (Linnaeus, 1758)
Alopoglossus atriventris Duellman, 1973
Alopoglossus bicolor (Werner, 1916), **new comb.**
Alopoglossus bilineatus (Boulenger, 1890), **new comb.**
Alopoglossus brevifrontalis (Boulenger, 1912), **new comb.**
Alopoglossus buckleyi (O'Shaughnessy, 1881)
Alopoglossus copii Boulenger, 1885
Alopoglossus danieli (Harris, 1994), **new comb.**
Alopoglossus embera Peloso and Hernandez-Morales, 2017
Alopoglossus eurylepis (Harris and Rueda, 1985), **new comb.**
Alopoglossus festae (Peracca, 1896)
Alopoglossus gorgonae (Harris, 1994), **new comb.**
Alopoglossus grandisquamatus (Rueda, 1985), **new comb.**
Alopoglossus kugleri (Roux, 1927), **new comb.**
Alopoglossus lehmanni Ayala and Harris, 1984
Alopoglossus meloi Ribeiro-Júnior, 2018
Alopoglossus myersi (Harris, 1994), **new comb.**
Alopoglossus harrisi, **new name.**
Alopoglossus plicatus (Taylor, 1949), **new comb.**
Alopoglossus romaleos (Harris, 1994), **new comb.**
Alopoglossus stenolepis (Boulenger, 1908), **new comb.**
Alopoglossus vallensis (Harris, 1994), **new comb.**
Alopoglossus viridiceps Torres-Carvajal and Lobos, 2014

Calyptommatus, *Dryadosaura*, *Anotosaura*, *Colobosauroides*, *Ameiva*, *Cnemidophorus*, *Dicrodon*, *Dracaena*, *Kentropyx* and *Teius*); (iv) the borders of the palatine process curved divergently and its distal tip truncated (in other Gymnophthalmoidea, this process has convergent or parallel borders according to Hernández-Morales et al., 2019); and (v) hemipenis without mineralized structures (Teiidae shows the same condition but most gymnophthalmids have mineralized structures in their hemipenis).

Comment on biogeography

Very little is known about the biogeography of Alopoglossidae, and we provide comments on the most striking biogeographic patterns that can be inferred from our analyses, and currently known distribution patterns of the species in the group. The vast majority of the known species in Alopoglossidae are found west of the Andes (Trans-Andean), with a few noteworthy exceptions. *Alopoglossus brevifrontalis* is exclusively Cis-Andean, found across most of the Amazon Basin (Peloso and Avila-Pires, 2010). *Alopoglossus bicolor* is restricted to the upper Rio Magdalena valley. *Alopoglossus harrisi* is found both on the western and eastern slopes of the Andes—Harris (1994) did mention some minor morphological differences between these two populations, but nonetheless considered them to be conspecific.

Torres-Carvajal and Lobos (2014) suggested a phylogenetic split between Cis-Andean and Trans-Andean taxa—their work considered only species then assigned to *Alopoglossus*, and did not include the Trans-Andean *A. lehmanni*. Peloso and Hernández-Morales (2017) named *A. embera* from the western slopes of the Andes but did not test its phylogenetic position. The authors, however, speculated about a close relationship between *A. embera*, *A. harrisi* (as *A. festae*), and *A. viridiceps* (Peloso and Hernández-Morales, 2017)—our phylogenetic analyses support this relationship. Also, our analyses support a split between Cis-Andean and Trans-Andean, if only the species formerly belonging to *Alopoglossus* are included. The Trans-Andean clade including *A. embera*, *A. harrisi*, and *A. viridiceps* is sister of the Cis-Andean clade including *A. angulatus*, and sister of the Cis-Andean clade including *A. angulatus*, *A. atriventris*, *A. buckleyi*, and *A. copii*. Collectively, both clades are sister of *A. lehmanni* (Trans-Andean).

Concluding remarks

This study is the first phylogenetic study to include all species of the Alopoglossidae. However, we also detected important gaps that will need to be addressed in the future. The position of the Alopoglossidae within Gymnophthalmoidea remains contentious—and so does the monophyly of Teiidae as currently defined. Moreover, future studies should improve on the sampling used here. It will be important to collect tissue samples for the species for which we do not have genomic data available, and further complete the morphological partition. Our morphological matrix of 143 characters was initially constructed based on previously published data, but a large number of new characters and character reappraisal were explored and incorporated. This matrix has the potential to be a baseline for future phylogenetic studies that incorporate morphological data not only on Alopoglossidae, but for the entire Gymnophthalmoidea.

Acknowledgments

We thank the American Museum of Natural History's Microscopy and Imaging Facility (H. Towbin and M. Hill), and the Nanoscale Research Facility at University of Florida (D. Blackburn and E. Stanley), for help with acquiring and processing CT images. The Geckolab at the Sam Houston State University (especially J. D. Daza) also helped with processing CT images. A. T. Galvis gave advice on the theoretical and operational issues of the implied weighting method. M. Bastos performed several of the anatomical preparations used here. We thank the curators and staff of the different collections that hold the specimens analyzed for their invaluable help: C. Raxworthy, D. Kizirian and L. Vonhamme (AMNH), W. Bolivar (CD-UV), A. Resetar (FMNH), R. Rios

(ICMN), M. Caderon (ICN), V. Paez (MHUA), A. Prudente (MPEG), K. de Queiroz (USNM), R. Sedano (UV-C), D. Blackburn (UF-FLMNH), E. la Marca (ULABG), and D. Rabosky (UMMZ). SL is most grateful to L. Mogk and G. Köhler (SMF) as well as to A. Batista and A. Hertz for their valuable logistical support. This study was financed in part by the Coordenação de Aperfeiçoamento de Pessoal de Nível Superior—Brasil (CAPES)—Finance Code 001. CHM was supported by a fellowship from Coordenação de Aperfeiçoamento de Pessoal de Nível Superior (CAPES), a Short-Term Visit Award by the Smithsonian Institution (we thank K. de Queiroz for acting as the sponsor for this grant) and the NSF award number 1657662. PLVP, MJS and PMSN were supported by Conselho Nacional de Desenvolvimento Cientíıfico e Tecnolóogico (CPNq research grant number 400252/2014-7; fellowship numbers 313680/2014-0; 313622/2018-3). PMSN was supported by Fundação de Amparo à Ciência do Estado de São Paulo (FAPESP fellowship numbers 2007/00811-8 and 2012/00492-8) and Fundação de Amparo à Ciência e tecnologia do Estado de Pernambuco (FACEPE research grant number APQ-0664-2.04/15). MJS was also supported by Coordenação de Aperfeiçoamento de Pessoal de Nível Superior. We thank all developers who make their software freely available, many of which were used herein.

References

Anaya-Rojas, J.M., Serrano-Cardozo, V.H., Ramirez-Pinilla, M.P., 2010. Diet, microhabitat use, and thermal preferences of *Ptychoglossus bicolor* (Squamata: Gymnophthalmidae) in an organic coffee shade plantation in Colombia. Pap. Avulsos Zool. 50, 159–166.

Arevalo, E.S., Davis, S.K., Sites, J.W., 1994. Mitochondrial DNA sequence divergence and phylogenetic relationships among eight chromosome races of the *Sceloporus grammicus* complex (Phrynosomatidae) in central Mexico. Syst. Biol. 43, 387–418.

Arteaga, A., Pyron, R.A., Pe, N., Romero-Barreto, P., Culebras, J., Bustamante, L., Yanez-Munuz, M., Guayasamin, J.M., 2016. Comparative phylogeography reveals cryptic diversity and repeated patterns of cladogenesis for amphibians and reptiles in northwestern Ecuador. PLoS ONE 11, e0151746.

Ayala, S.C., Harris, D.M., 1984. A new microteiid lizard (*Alopoglossus*) from the Pacific rainforest of Colombia. Herpetologica 40, 154–158.

Benson, D.A., Cavanaugh, M., Clark, K., Karsch-Mizrachi, I., Lipman, D.J., Ostell, J., Sayers, E.W., 2013. GenBank. Nucleic Acids Res. 41, 36–42.

Bolívar-G, W., Hernandez-Morales, C., 2013. *Ptychoglossus stenolepis* (Boulenger 1908). Catalogo de Anfibios y Reptiles de Colombia 1, 26–30.

Bonnaterre, P.J., 1789. Tableau encyclopédique et méthodique des trois règnes de la nature. Erpétologie. Panckoucke, Paris.

Boulenger, G.A., 1885. Catalogue of the lizards in the British Museum (Natural History). II. Iguanidae, Xenosauridae, Zonuridae, Anguidae, Anniellidae, Helodermatidae, Varanidae, Xantusiidae, Teiidae, Amphisbaenidae. Taylor & Francis, London.

Boulenger, G.A., 1890. First report on additions to the lizard collection in the British Museum (Natural History). Proc. Zool. Soc. Lond. 1890, 77–86.

Boulenger, G.A., 1908. Descriptions of new batrachians and reptiles discovered by Mr. M. G. Palmer in south-western Colombia. Ann. Mag. Nat. Hist. Ser. 8, 515–522.

Boulenger, G.A., 1912. Descriptions of new batrachians from the Andes of South America, preserved in the British Museum. Ann. Mag. Nat. Hist. Ser. 8, 185–191.

Bremer, K., 1988. The limits of amino acid sequence data in angiosperm phylogenetic reconstruction. Evolution 42, 795–803.

Castoe, T., Doan, T., Parkinson, C., 2004. Data partitions and complex models in Bayesian analysis: the phylogeny of gymnophthalmid lizards. Syst. Biol. 53, 448–469.

Colli, G.R., Hoogmoed, M.S., Cannatella, D.C., Cassimiro, J., Gomes, J.O., Ghellere, J.M., Nunes, P.M.S., Pellegrino, K., Salerno, P., De Souza, S.M., Rodrigues, M.T. 2015. Description and phylogenetic relationships of a new genus and two new species of lizards from Brazilian Amazonia, with nomenclatural comments on the taxonomy of Gymnophthalmidae (Reptilia: Squamata). Zootaxa 4000, 401–427.

Conrad, J.L., 2008. Phylogeny and systematics of Squamata (Reptilia) based on morphology. Bull. Am. Mus. Nat. Hist. 310, 1–182.

Cope, E.D., 1875. Report on the Reptiles brought by Professor James Orton from the middle and upper Amazon and western Peru. J. Acad. Nat. Sci. Phila. 2, 159–183.

Duellman, W.E., 1973. Descriptions of new lizards from the upper Amazon basin. Herpetologica 29, 228–231.

Duméril, A.M.C., Bribon, G., 1839. Erpétologie Générale on Histoire Naturelle Complète des Reptiles, Vol. 5. Roret/Fain et Thunot, Paris.

Gauthier, J.A., Kearney, M., Maisano, J.A., Rieppel, O., Behlke, A.D.B., 2012. Assembling the squamate tree of life: perspectives from the phenotype and the fossil record. Bull. Peabody Mus. Nat. Hist. 53, 3–308.

Giribet, G., Wheeler, W.C., 2007. The case for sensitivity: a response to Grant and Kluge. Cladistics 23, 294–296.

Giribet, G., DeSalle, R., Wheeler, W.C., 2002. 'Pluralism' and the aims of phylogenetic research. In: DeSalle, R., Giribet, G., Wheeler, W.C. (Eds.), Molecular Systematics and Evolution: Theory and Practice. Birkhäuser Verlag, Basel, pp. 141–146.

Goicoechea, N., Frost, D.R., De la Riva, I., Pellegrino, K.C.M., Sites, J., Rodrigues, M.T. and Padial, J.M., 2016. Molecular systematics of teioid lizards (Teioidea: Gymnophthalmoidea: Squamata) based on the analysis of 48 loci under tree-alignment and similarity. Cladistics 32, 1–48.

Goloboff, P.A., 1993. Estimating character weights during tree search. Cladistics 9, 83–91.

Goloboff, P., 1999. Analyzing large data sets in reasonable times: solution for composite data. Cladistics 15, 70–79.

Goloboff, P.A., 2008. Calculating SPR distances between trees. Cladistics 24, 591–597.

Goloboff, P.A., 2014. Extended implied weighting. Cladistics 30, 260–272.

Goloboff, P.A., Farris, J.S., Källersjö, M., Oxelman, B., Ramirez, M.J., Szumik, C.A., 2003. Improvements to resampling measures of group support. Cladistics 19, 324–332.

Goloboff, P.A., Farris, J.S., Nixon, K.C., 2008. TNT, a free program for phylogenetic analysis. Cladistics 24, 774–786.

Goodman, M., Olson, C.B., Beeber, J.E., Czelusniak, J., 1982. New perspectives in the molecular biological analysis of mammalian phylogeny. Acta Zool. Fennica 169, 19–35.

Grant, T., Kluge, A.G., 2005. Stability, sensitivity, science and heurism. Cladistics 21, 597–604.

Grant, T., Kluge, A.G., 2008. Credit where credit is due: the Goodman-Bremer support metric. Mol. Phylog. Evol. 49, 405–406.

Gray, J.E., 1825. A synopsis of the genera of reptiles and amphibians, with a description of some new species. Ann. Phil. 10, 193–217.

Gray, J.E., 1827. Synopsis of the genera of saurian reptiles, in which some new genera are indicated, and the others reviewed by actual examination. Philos. Mag. Ann. Chem. 2, 54–58.

Gray, J.E., 1851. Description of a new genus and family of cyclosaurian lizards, from Para. Proc. Zool. Soc. Lond. 19, 38–39.

Harris, D.M., 1985. Infralingual plicae: support for Boulenger's Teiidae (Sauria). Copeia 1985, 560–565.

Harris, D.M., 1994. Review of the teiid lizard genus *Ptychoglossus*. Herpetol. Monogr. 8, 226–275.
Harris, D.M., Rueda, J.V., 1985. A new microteiid lizard (Sauria: *Ptychoglossus*) with exceptionally wide scales from southwestern Colombia. Acta Biol. Colomb. 48, 1–6.
Hernandez-Morales, C., Peloso, P.L.V., Bolivar-G, W., Daza, J.D. 2019. Skull morphology of the lizard *Ptychoglossus vallensis* (Squamata: Alopoglossidae) with comments on the variation within Gymnophthalmoidea. Anat. Rec. 302, 1074–1092.
Hoyos, J.M., 1998. A reappraisal of the phylogeny of lizards of the family Gymnophthalmidae (Sauria, Scincomorpha). Rev. Esp. Herpetol. 12, 27–43.
Katoh, K., Kuma, K., Toh, H., Miyata, T., 2005. MAFFT, a novel method for rapid multiple sequence alignment based on fast Fourier transform. Nucleic Acids Res. 30, 3059–3066.
Kearse, M., Moir, R., Wilson, A., Stones-Havas, S., Cheung, M., Sturrock, S., Buxton, S., Cooper, A., Markowitz, S., Duran, C., Thierer, T., Ashton, B., Meintjes, P., Drummond, A., 2012. Geneious basic: an integrated and extendable desktop software platform for the organization and analysis of sequence data. Bioinformatics 28, 1647–1649.
Kocher, T.D., Thomas, W.K., Meyer, A., Edwars, S.V., Paabo, S., Villablanca, F.X., Wilson, A.C., 1989. Dynamics of mitochondrial DNA evolution in animals: amplification and sequencing with conserved primers. Proc. Natl. Acad. Sci. USA 86, 6196–6200.
Köhler, G., Diethert, H.-H., Veselý, M., 2012. A contribution to the knowledge of the lizard genus *Alopoglossus* (Squamata: Gymnophthalmidae). Herpetol. Monogr., 26, 173–188.
Laurenti, J.N., 1768. Specimen medicum, exhibens synopsin reptilium emendatam cum experimentis circa venena et antidota reptilium austracorum, quod authoritate et consensu, 2nd ed. Joan Thomae, Vienna.
van Lidth de Jeude, T.W., 1904. Reptiles and batrachians from Surinam. Notes Leyden Mus. 25, 83–94.
Linnaeus, C., 1758. Systema Naturae per Regna Tria Naturae, Secundum Classes, Ordines, Genera, Species, cum Characteribus, Differentiis, Synonymis, Locis, 10th ed., Vol. 1. Laurentii Salvii, Holmiae, Sweden.
Machado, D.J., 2015. YBYRÁ facilitates comparison of large phylogenetic trees. BMC Bioinform. 16, 204.
MacLean, R.R., 1974. Feeding and locomotor mechanisms of teiid lizards: functional morphology and evolution. Pap. Avulsos Zool. 27, 179–213.
Maddison, W.P., Maddison, D.R., 2010. Mesquite: a modular system for evolutionary analysis, version 3.04. http://mesquite-project.org
Maisano, J.A., 2008. A protocol for clearing and double-staining squamate specimens. Herpetol. Rev. 39, 52–54.
Meza-Joya, F.L., Ramos-Pallares, E., Hernández-Jaimes, C.A., 2014. *Ptychoglossus bicolor* (Werner 1916). Catalogo de Anfibios y Reptiles de Colombia 2, 24–29.
Mirande, J., 2009. Weighted parsimony phylogeny of the family Characidae (Teleostei: Characiformes). Cladistics 25, 574–613.
Nixon, K.C., 1999. The parsimony ratchet, a new method for rapid parsimony analysis. Cladistics 15, 407–414.
O'Shaughnessy, A.W.E., 1881. An account of the collection of lizards made by Mr. Buckley in Ecuador, and now in the British Museum, with descriptions of the new species. Proc. Zool. Soc. Lond. 49, 227–245.
Pellegrino, K.C.M., Rodrigues, M.T., Yonenaga-Yassuda, Y., Sites, J.W.J., 2001. A molecular perspective on the evolution of microteiid lizards (Squamata, Gymnophthalmidae), and a new classification for the family. Biol. J. Linnean Soc. 74, 315–338.
Peloso, P.L.V., Avila-Pires, T.C.S., 2010. Morphological variation in *Ptychoglossus brevifrontalis* Boulenger, 1912 and the status of *Ptychoglossus nicefori* (Loveridge, 1929) (Squamata, Gymnophthalmidae). Herpetologica 66, 357–372.
Peloso, P.L.V., Hernandez-Morales, C., 2017. Description of a new species of *Alopoglossus* Boulenger, 1885 from western Colombia (Gymnophthalmoidea). South Am. J. Herpetol. 12, 89–98.
Peloso, P.L., Pellegrino, K.C.M., Rodrigues, M.T., Ávila-Pires, T.C.S., 2011. Description and phylogenetic relationships of a new genus and species of lizard (Squamata, Gymnophthalmidae) from the Amazonian rainforest of northern Brazil. Am. Mus. Novit. 3713, 1–24.
Peracca, M.G., 1896. Descrizione di un nuevo genere e di una nuova specie di Teiidae raccolta nel Darien dal dott. E. Festa. Boll. Mus. Zool. Anat. Comp. Univ. Torino. 11, 1–4.
Peracca, M.G., 1904. Rettili ed anfibi. Boll. Mus. Zool. Anat. Comp. Univ. Torino. 19, 1–41.
Pesantes, O.S., 1994. A method for preparing the hemipenis of preserved snakes. J. Herpetol. 28, 93–95.
Presch, W., 1980. Evolutionary history of the South American microteiid lizards (Teiidae: Gymnophthalmidae). Copeia 1980, 36–56.
Pyron, R.A., Burbrink, F.T., Wiens, J.J., 2013. A phylogeny and revised classification of Squamata, including 4161 species of lizards and snakes. BMC Evol. Biol. 13, 1–53.
Reeder, T.W., Townsend, T.M., Mulcahy, D.G., Noonan, B.P., Wood, P.L., Sites, J.W., Wiens, J.J. 2015. Integrated analyses resolve conflicts over squamate reptile phylogeny and reveal unexpected placements for fossil taxa. PLoS ONE 10, 1–22.
Reemer, M., Ståhls, G., 2013. Phylogenetic relationships of Microdontinae (Diptera: Syrphidae) based on molecular and morphological characters. Syst. Entomol. 38, 661–688.
Reinhardt, J., Lütken, C., 1862. Bidrag til Kundskab om Brasiliens Padder og Krybdyr. Förste Afdeling Paddern og Oglerne. Vidensk. Medd. Dansk Naturhist. Foren. Kjobenhavn. 1861, 143–242.
Ribeiro-Júnior, M.A., 2018. A new species of *Alopoglossus* lizard (Squamata, Alopoglossidae) from the southern Guiana Shield, northeastern Amazonia, with remarks on diagnostic characters to the genus. Zootaxa 4422, 25–40.
Rieppel, O. (1984) Miniaturization of the lizard skull: its functional and evolutionary implications. In: Ferguson, M.W. (Ed.) The Structure, Development and Evolution of Reptiles. New York: Symposia of the Zoological Society of London, pp. 503–520.
Rieppel, O., Gauthier, J., Maisano, J., 2008. Comparative morphology of the dermal palate in squamate reptiles, with comments on phylogenetic implications. Zool. J. Linnean Soc. 152, 131–152.
Rodrigues, M.T., Freire, E.M.X., Pellegrino, K.C.M., Sites, J.W. Jr, 2005. Phylogenetic relationships of a new genus and species of microteiid lizard from the Atlantic forest of north-eastern Brazil (Squamata, Gymnophthalmidae). Zool. J. Linnean Soc. 144, 543–557.
Rodrigues, M.T., Machado, K.C., Dixo, M., Verdade, V.K., Sites, J.W., 2007. A new genus of microteiid lizard from the Atlantic Forests of state of Bahia, Brazil, with a new generic name for *Colobosaura mentalis*, and a discussion of relationships among the Heterodactylini (Squamata, Gymnophthalmidae). Am. Mus. Novit. 3565, 1–27.
Rodrigues, M.T., Cassimiro, J., Pavan, D., 2009. A new genus of microteiid lizard from the Caparaó mountains, southeastern Brazil, with a discussion of relationships among Gymnophthalminae (Squamata). Am. Mus. Novit. 3673, 1–28.
Roscito, J.G., Rodrigues, M.T., 2010. Comparative cranial osteology of fossorial lizards from the tribe Gymnophthalmini (Squamata, Gymnophthalmidae). J. Morphol. 271, 1352–65.
Roscito, J.G., Nunes, P.M.S., Rodrigues, M.T., 2014. Digit evolution in gymnophthalmid lizards. Int. J. Dev. Biol. 58, 895–908.
Roux, J., 1927. Contribution a l'erpetologie du Venezuela. Verhandl. Naturforsch. Ges. Basel. 38, 252–261.
Rueda, J.V., 1985. Acerca de las especies colombianas del genero *Ptychoglossus* (Sauria: Gymnophthalmidae) con la descripción de una nueva especie. Lozania 51, 1–12.
Ruibal, R., 1952. Revisionary studies of some South American Teiidae. Bull. Mus. Comp. Zool. 106, 477–529.
Ruthven, A.G., 1916. Description of a new genus and species of lizard from British Guiana. Occ. Pap. Mus. Zool. Univ. Michigan. 2, 151–196.
Saint, K.M., Austin, C.C., Donnellan, S.C., Hutchinson, M.N., 1998. C-mos, a nuclear marker useful for squamate phylogenetic analysis. Mol. Phylogenet. Evol. 10, 259–263.
von Spix, J.B., 1825. Animalia Nova sive species novae Lacertarum, quas in itinere per Brasiliam annis MDCCCXVII-MDCCCXX jussu et auspiciis Maximiliani Josephi I. Bavariae regis suscepto collegit et descripsit Dr. J. B. de Spix.

Taylor, E.H., 1949. Two new teiid lizards from Costa Rica. Univ. Kansas Sci. Bull. 33, 271–278.
Torres-Carvajal, O., Lobos, S.E., 2014. A new species of *Alopoglossus* lizard (Squamata, Gymnophthalmidae) from the tropical Andes, with a molecular phylogeny of the genus. ZooKeys 120, 105–120.
Uetz, P., Hallerman, J., 2014. The reptile database. http://www.reptile-database.org/. Accessed in September, 2018.
Vaidaya, G., Lohman, D.J., Meier, R., 2011. SequenceMatrix: concatenation software for the fast assembly of multi-gene datasets with character set and codon information. Cladistics 27, 171–180.
Wagler, J.G., 1830. Natürliches System der Amphibien, mit vorangehender Classification der Säugthiere und Vögel. J.G. Cotta, Stuttgart und Tübingen, Deutschland.
Werner, F., 1916. Bemerkungen über einige niedere Wirbeltiere der Anden von Kolumbien mit Beschreibungen neuer Arten. Zool. Anz. 47, 301–304.
Wheeler, W.C., 1995. Sequence alignment, parameter sensitivity, and the phylogenetic analysis of molecular data. Syst. Biol. 44, 321–331.
Wheeler, W.C., 1996. Optimization alignment: the end of multiple sequence alignment in phylogenetics? Cladistics 12, 1–9.
Zaher, H., Prudente, A., 2003. Hemipenes of *Siphlophis* (Serpentes, Xenodontinae) and techniques of hemipenial preparation in snakes: a response to Dowling. Herpetol. Rev. 34, 302–307.

Supporting Information

Additional supporting information may be found online in the Supporting Information section at the end of the article.

Appendix S1. List of examined material.

Appendix S2. Taxon sampling, including the complete list of species in the dataset, and showing which one has information for each partition of data.

Appendix S3. Summary of SPR distance and bootstrap support values for alternative weighting schemes used in the sensitivity analysis.

Appendix 1

Morphological characters

Tongue (n = 5)

1. Cover of the dorsal surface of the tongue: (0) entirely covered by oblique plicae; (1) covered by oblique plicae proximally and by scale-like papillae distally; (2) entirely covered by scale-like papillae (Boulenger, 1885; Fig. 3).
2. Tongue papillae arrangement: (0) juxtaposed; (1) imbricated.
3. Sublingual plicae: (0) absent; (1) present (Harris, 1985).
4. Longitudinal sulcus on the middle part of the tongue: (0) absent; (1) present.
5. Pigmentation of the tongue: (0) entirely light; (1) entirely dark; (2) light proximally and dark distally.

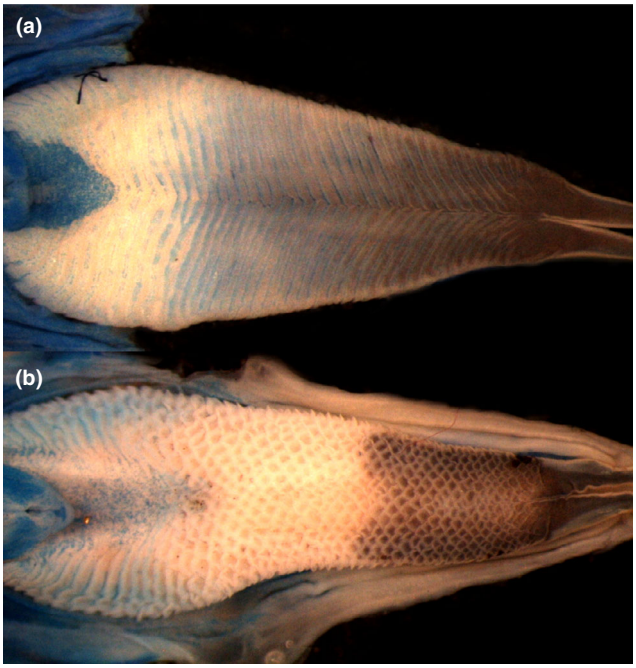

Fig. 3. Dorsal view of the tongue of (a) *Alopoglossus angulatus* (MPEG 15151) and (b) *Cercosaura ocellata* (MPEG 29372). [Colour figure can be viewed at wileyonlinelibrary.com]

Scutellation (n = 68)

6. Eyelid: (0) absent; (1) present.
7. Proportion of the frontonasal: (0) wider than long; (1) longer than wide or approximately equal sides.
8. Prefrontal scales: (0) absent; (1) present.
9. Contact between prefrontals: (0) absent; (1) present.
10. Nasal divided: (0) entire; (1) divided.
11. Nasal scales division: (0) two scales; (1) three scales.
12. Nasal scale configuration: (0) in contact; (1) separated from each other by the rostral and frontonasal scales.
13. Nostril position: (0) lateral; (1) lateroposterior (Köhler et al., 2012).
14. Frontoparietal scales: (0) absent; (1) present.
15. Supraocular count: (0) three; (1) four; (2) two.
16. Size of second supraocular: (0) similar in size to third supraocular; (1) twice the size of third supraocular.
17. Posterior border of the parietal and interparietal scales: (0) form a nearly straight suture across the back of the head; (1) form an irregular suture across the back of the head; (2) form a rounded suture across the back of the head.
18. Interparietal: (0) absent; (1) present.
19. Interparietal divided: (0) entire; (1) divided.
20. Size of interparietal: (0) similar in size to the parietals; (1) smaller than parietals; (2) larger than parietals (Fig. 4).

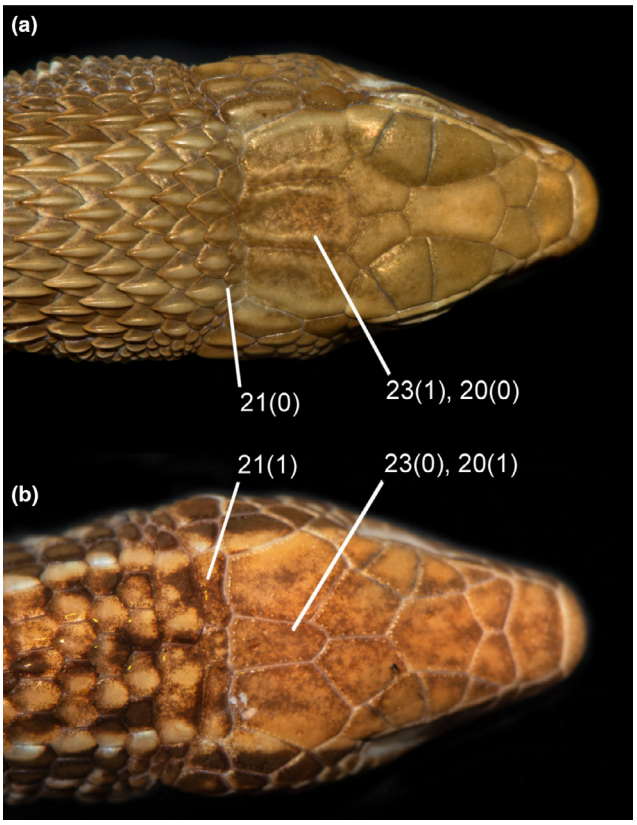

Fig. 4. Dorsal view of the head and neck region in (a) *Alopoglossus festae* (AMNH 110610) and (b) *Ptychoglossus festae* (KU 76176). [Colour figure can be viewed at wileyonlinelibrary.com]

21. Exceptionally broad scales forming occipital scale rows: (0) absent; (1) present (Harris, 1994; Fig. 4).
22. Two enlarged longitudinal rows of scales on the nape: (0) absent; (1) present.
23. Ornamentation of the parietal scales: (0) absent; (1) present (Fig. 4).
24. Type of ornamentation of the parietals: (0) ridged; (1) irregular surface.
25. Ornamentation of the frontoparietal scales: (0) absent; (1) present.
26. Type of ornamentation of the frontoparietals: (0) ridged; (1) irregular surface.
27. Ornamentation on the frontal scale: (0) absent; (1) present.
28. Type of ornamentation of the frontal: (0) ridged; (1) irregular surface.
29. Tympanic recess: (0) absent; (1) present.
30. Ornamentation of temporal scales: (0) smooth; (1) keeled.
31. Loreals: (0) unique; (1) divided, more than one.
32. Frenocular in contact with the nasal anteriorly: (0) absent; (1) present.
33. Pairs of enlarged chin shields: (0) three; (1) two; (2) one; (3) six (4) five; (5) four.
34. Number of infralabials in contact with chinshields (per side): (0) 4; (1) 5; (2) 6; (3) 3.
35. Third chinshields separated from infralabials: (0) absent; (1) present.
36. Third chinshields separated from infralabials by: (0) one sublabial; (1) two sublabials; (2) granular scales.
37. Third pair of chinshields in contact medially: (0) absent; (1) present (Fig. 5).
38. Second pair of chinshields in contact medially: (0) absent; (1) present (Fig. 5).
39. Gular crease: (0) absent; (1) present.
40. Guttural fold: (0) absent; (1) present.
41. Pregulars differentiated from the gulars: (0) absent; (1) present.
42. Pregular scale shape: (0) plate-like; (1) granular; (2) granular medially and plate-like laterally; (3) with a pair of enlarged scales medially (Fig. 5).
43. Pregular scale arrangement: (0) juxtaposed; (1) imbricated.
44. Widened paramedian plates: (0) absent; (1) present (Fig. 5).
45. Lateral neck scales: (0) totally plate-like; (1) totally granular; (2) granular anteriorly and plate-like posteriorly; (3) longitudinal rows of granular scales between rows of enlarged scales.
46. When plate-like, lateral neck scales: (0) round; (1) quadrangular; (2) lanceolate; (3) cycloid.
47. Ornamentation of the lateral neck scales: (0) smooth; (1) keeled; (2) only keeled on the posterior part of the neck.
48. Dorsal scale rows: (0) more evidently disposed in transversal rows; (1) disposed in transversal and oblique rows.
49. Arrangement of dorsal scales with respect to the anteriorly and posteriorly adjacent scales: (0) juxtaposed; (1) imbricated; (2) longitudinal rows of juxtaposed scales between rows of imbricated scales.
50. Arrangement of dorsal scales with respect to the laterally adjacent scales: (0) juxtaposed; (1) imbricated.
51. Dorsal scale shape: (0) rectangular; (1) squared; (2) mucronate; (3) granular; (4) pentagonal; (5) cycloid; (6) rows of mucronate and rows of granular scales.
52. Ornamentation of dorsal scales: (0) smooth; (1) keeled; (2) rows of smooth and rows of keeled scales.
53. Well-defined paravertebral scale rows: (0) absent; (1) present.
54. Posterior border of the ventral scales: (0) truncated; (1) mucronate; (2) angulated; (3) rounded (Fig. 6).
55. Posterior border of infracaudals: (0) truncated; (1) angulated; (2) rounded; (3) mucronate.
56. Arrangement of ventral scales with respect to the laterally adjacent scales: (0) juxtaposed; (1) imbricate.
57. Ornamentation of ventral scales: (0) smooth; (1) keeled (Fig. 6).
58. Lateral fold: (0) absent; (1) present.

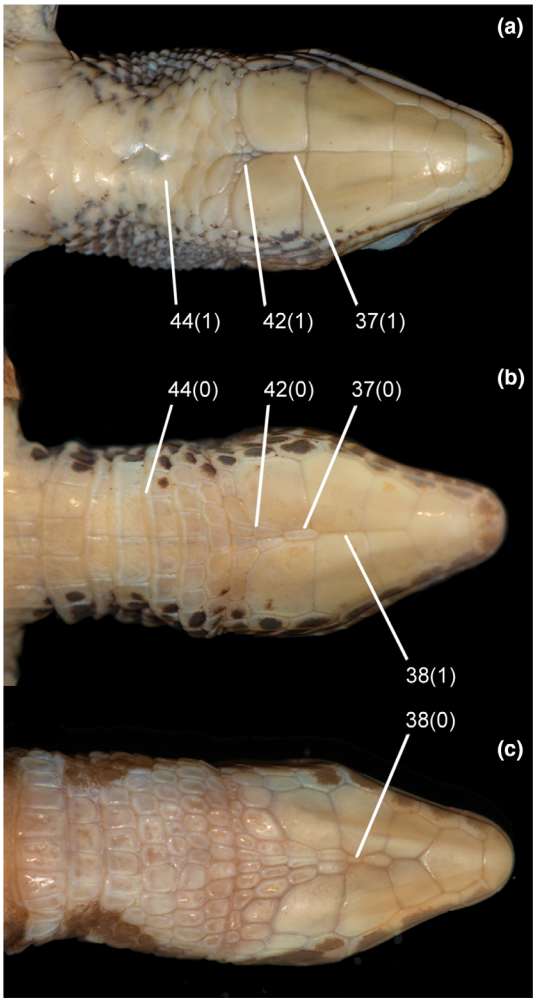

Fig. 5. Ventral view of the head in (a) *Alopoglossus festae* (AMNH 110610), (b) *Ptychoglossus festae* (KU 76176), and (c) *Ptychoglossus gorgonae* (UMMZ 171669). [Colour figure can be viewed at wileyonline library.com]

59. Transversal rows of scales on lateral fold: (0) absent; (1) present.
60. Precloacal pores in males: (0) absent; (1) present.
61. Precloacal pores in females: (0) absent; (1) present.
62. When precloacal pore series present: (0) at the same level where they come together; (1) staggered behind the femoral pore series.
63. Femoral pores in males: (0) absent; (1) present.
64. Femoral pores in females: (0) absent; (1) present.
65. Scales bearing femoral pores: (0) entire; (1) divided.
66. Scales bearing precloacal pores: (0) entire; (1) divided.
67. Thenar scale size: (0) small; (1) enlarged (Harris, 1994).
68. Ornamentation of dorsal scales of the arm: (0) smooth; (1) keeled.
69. Ornamentation of the scales on anterior surface of thigh: (0) smooth; (1) keeled.

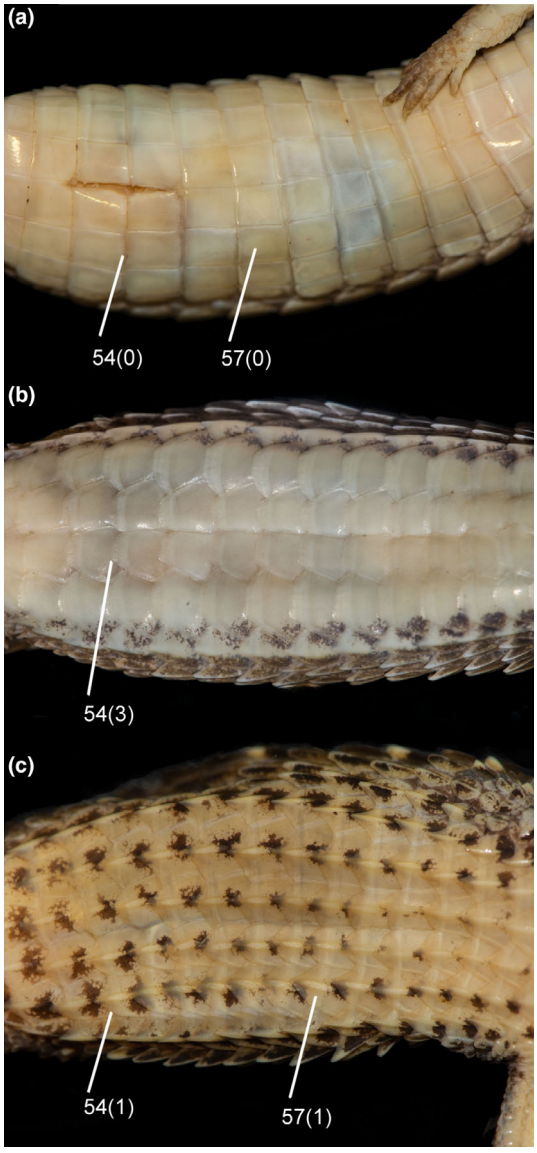

Fig. 6. Ventral view of abdominal region in (a) *Ptychoglossus kugleri* (MCZ 48912), (b) *Alopoglossus festae* (AMNH 110610), and (c) *Alopoglossus copii* (KU 222169). [Colour figure can be viewed at wileyon linelibrary.com]

70. Ornamentation of the scales on posterior surface of the thigh: (0) smooth; (1) keeled.
71. Ornamentation of the anterior part of the bobbin: (0) smooth; (1) keeled.
72. Ornamentation of subcaudal scales: (0) smooth; (1) keeled.
73. Ornamentation of supracaudal scales: (0) smooth; (1) keeled.

Hemipenis (n = 10)

74. Hemipenis with mineralized spines: (0) absent; (1) present.

75. Hemipenis with comb-like spicules: (0) absent; (1) present.
76. Hemipenis shape: (0) cylindrical; (1) the proximal part narrow, turning wider gradually in distal direction (P. M. S. Nunes, unpublished data).
77. Hemipenis distally forked: (0) absent; (1) present.
78. Hemipenial capitulum: (0) absent; (1) present.
79. Hemipenis with odd projections on the distal tip of the capitulum: (0) absent; (1) present.
80. Ornamentation of the distal region of the hemipenis: (0) symmetrical; (1) asymmetrical (Harris, 1994; P. M. S. Nunes, unpublished data).
81. Flounces of the hemipenis: (0) absent; (1) present.
82. Direction of the hemipenial flounces on the asulcated face: (0) perpendicular in relation to the longitudinal axis of the hemipenis; (1) oblique in relation to the longitudinal axis of the hemipenis.
83. Spermatic sulcus obliterated distally: (0) absent; (1) present (P. M. S. Nunes, unpublished data).

Cranium (n = 39)

84. Relation among neurocranium and dermatocranium: (0) dermatocranium and neurocranium located at different levels, with a larger post-temporal fenestrae; (1) dermatocranium and neurocranium located at the same level, obliterating the post-temporal fenestrae (Rieppel, 1985; Fig. 7).
85. Maximum number of dental cuspids in maxillary teeth: (0) 1; (1) 2; (2) 3.
86. Like molar teeth: (0) absent; (1) present.
87. Pterygoid teeth: (0) absent; (1) present (Harris, 1994; Fig. 8).

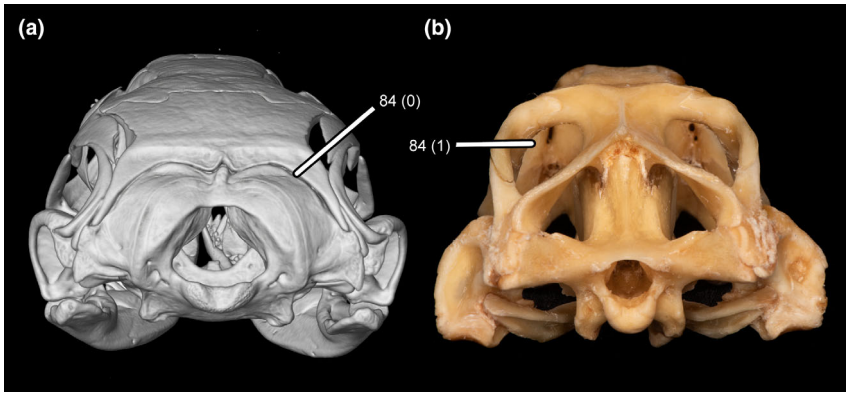

Fig. 7. Posterior view of the skull in (a) *Ptychoglossus vallensis* (AMNH 119239), and (b) *Salvator merianae* (CEPB 10888). [Colour figure can be viewed at wileyonlinelibrary.com]

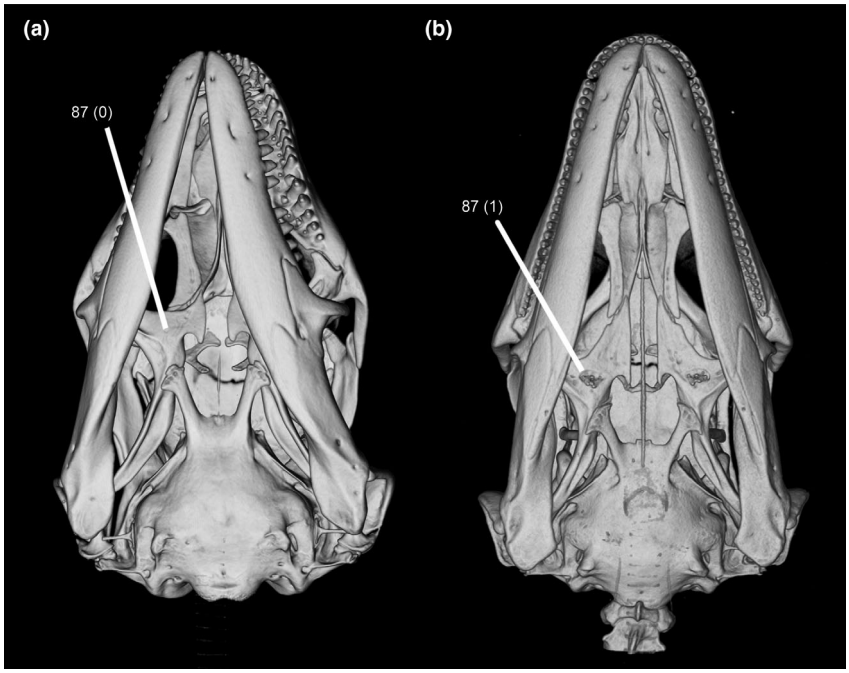

Fig. 8. Ventral view of the skull in (a) *Ptychoglossus vallensis* (AMNH 119239), and (b) *Alopoglossus buckleyi* (AMNH 113762).

88. Breadth of the dorsal process of the premaxilla: (0) smaller than premaxillary teeth row; (1) similar to premaxillary teeth row (Fig. 9).
89. Basal part of the dorsal process of the premaxilla: (0) with basal constriction, that constriction is strong and abrupt; (1) without basal constriction (Fig. 10).
90. Contact between the nasals: (0) absent; (1) present (Fig. 11).
91. The contact between the dorsal surface of the posterior process of the maxilla and the suborbital process of the jugal visible laterally: (0) absent, covered by the posterior part of the facial process of the maxilla; (1) present (Fig. 12).
92. The relation between the palatal shelf and the vomer: (0) palaeochoanate condition; (1) incomplete neochoanate condition; (2) neochoanate condition; (3) duplicipalatine (Rieppel et al., 2008).
93. In the maxilla, width of the palatal shelf: (0) relatively the same through all of the palatal shelf; (1) abrupt reduction of the palatal shelf at its mid-point; (2) palatal shelf disappears after the midpoint of the dental row.
94. Interorbital constriction of the frontal: (0) half as wide as the posterior part of the frontal; (1) a third as wide as the posterior part of the frontal; (2) only slightly more narrow than the posterior part of the frontal.
95. Frontoparietal tabs: (0) with the same or less length of the parietal processes of the frontal; (1) taller than the parietal processes of the frontal; (2) without frontoparietal tabs (MacLean, 1974; Presch, 1980; Fig. 13).
96. *Cristae cranii*: (0) forming lateral descending ridges; (1) forming a tubular structure (MacLean, 1974; Presch, 1980; Fig. 14).
97. Parietal proportions, this considering the length from the posterior part of the posteromedial slit

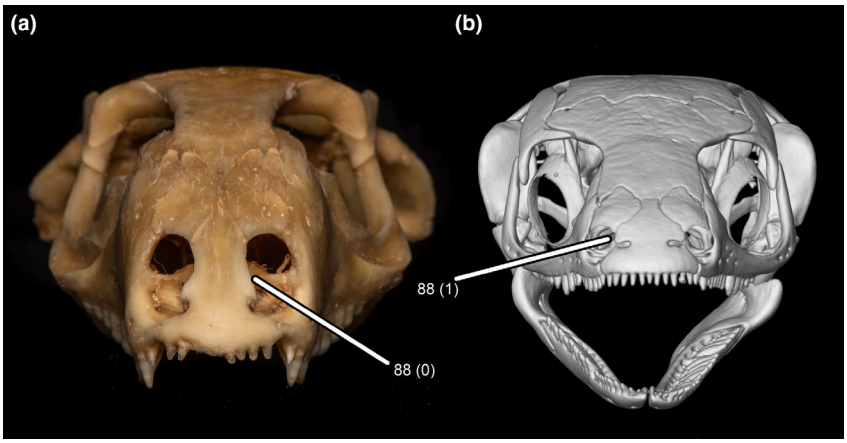

Fig. 9. Frontal view of skull (snout) in (a) *Salvator merianae* (CEPB 10888), and (b) *Ptychoglossus vallensis* (AMNH 119239). [Colour figure can be viewed at wileyonlinelibrary.com]

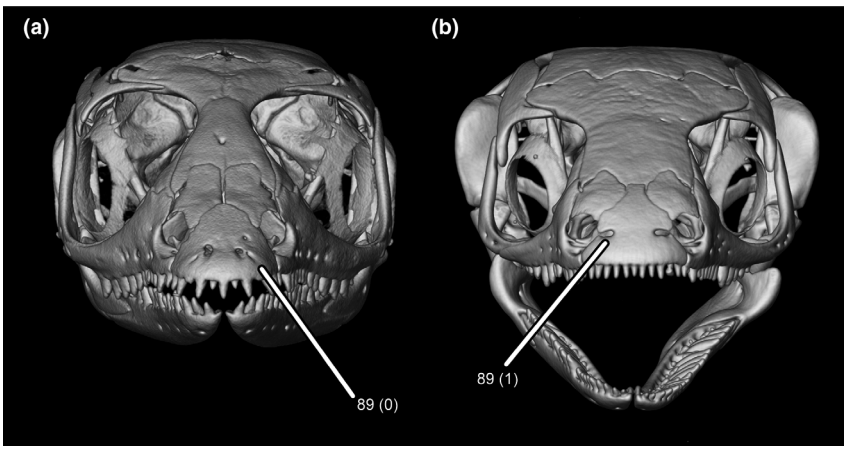

Fig. 10. Frontal view of skull in (a) *Loxopholis guianense* (HERR 15357), and (b) *Ptychoglossus vallensis* (AMNH 119239).

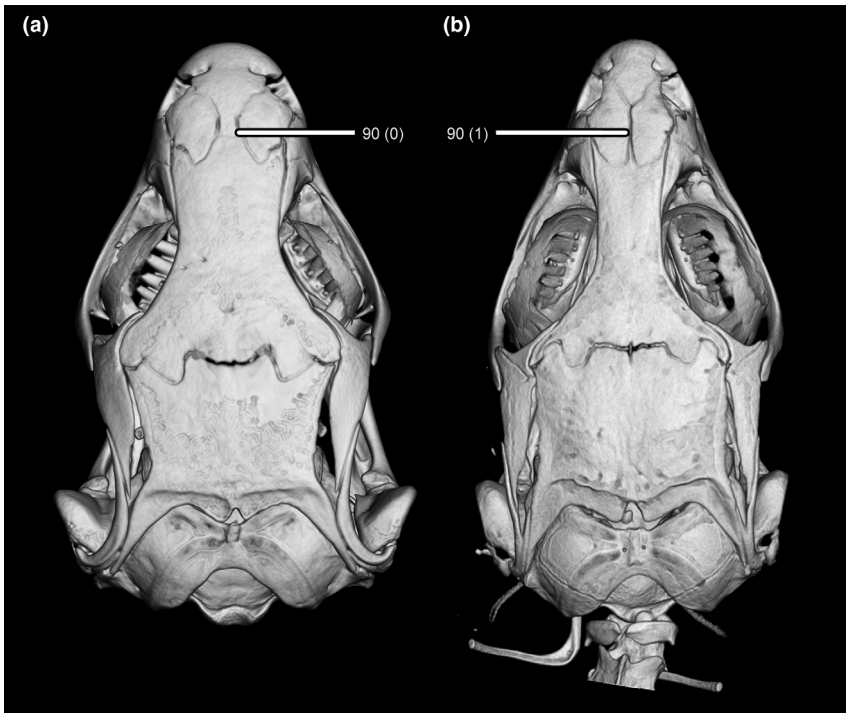

Fig. 11. Dorsal view of the skull in (a) *Ptychoglossus vallensis* (AMNH 119239), and (b) *Loxopholis guianense* (HERR 15357).

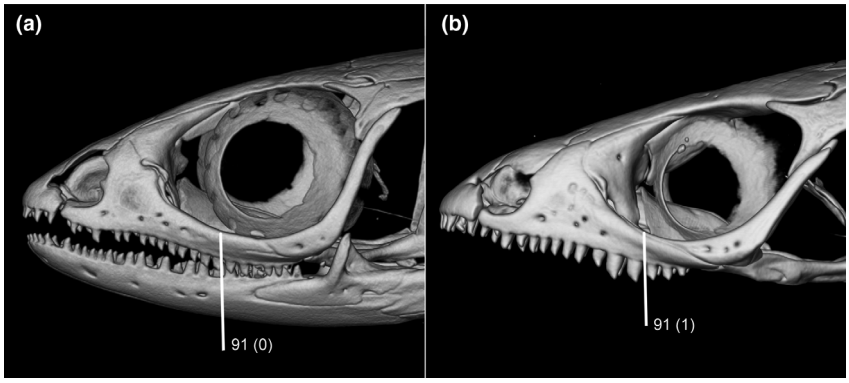

Fig. 12. Lateral view of the anterior portion of the skull in (a) *Loxopholis guianense* (HERR 15357), and (b) *Ptychoglossus vallensis* (AMNH 119239).

to the contact border with the frontal, and the width between the dorsal edges of the supratemporal fenestrae: (0) wider than long; (1) longer than wide.

98. Lateral borders of the body of parietal: (0) straight; (1) slightly curved medially; (2) strongly curved medially.
99. Lateral shelf of the parietal: (0) absent; (1) present.
100. Sagittal crest on the parietal: (0) absent; (1) present.
101. Parietal flat: (0) absent, dorsally convex; (1) present.
102. The descending ventral process of the parietal: (0) small, occupying only the superior part of the infratemporal fenestra; (1) hypertrophied (Roscito and Rodrigues, 2010; Fig. 15).
103. The posterolateral processes of the parietal proportions: (0) the length is similar to the lateral edge of the parietal body; (1) longer than the lateral edges of the parietal body; (2) reduced.
104. Posterolateral process of the parietal shape: (0) laterally flat; (1) vertically flat.
105. Foramen pineale: (0) absent; (1) present.

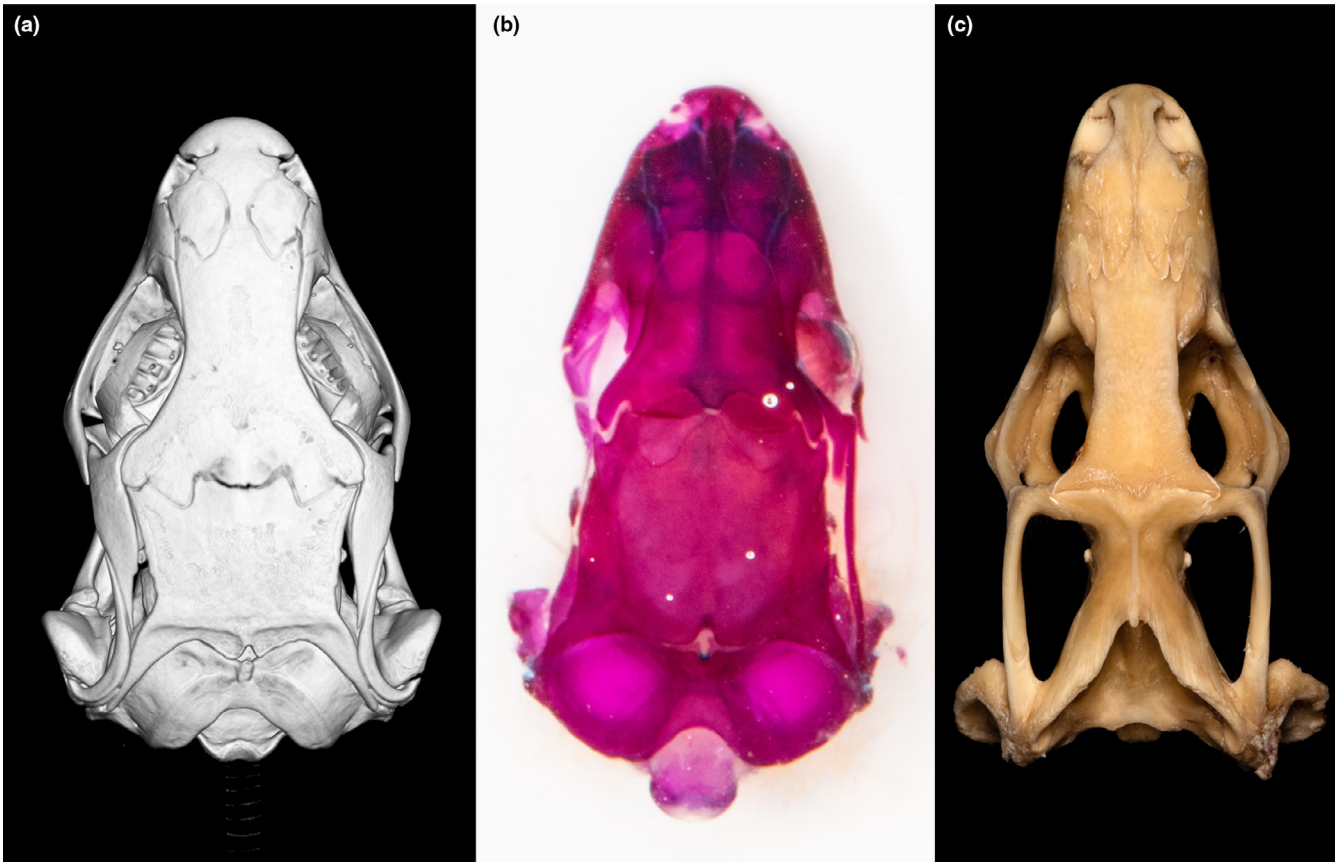

Fig. 13. Dorsal view of the skull in (a) *Ptychoglossus vallensis* (AMNH 119239), (b) *Bachia flavescens* (MPEG 27586), and (c) *Salvator merianae* (CEPB 10888). [Colour figure can be viewed at wileyonlinelibrary.com]

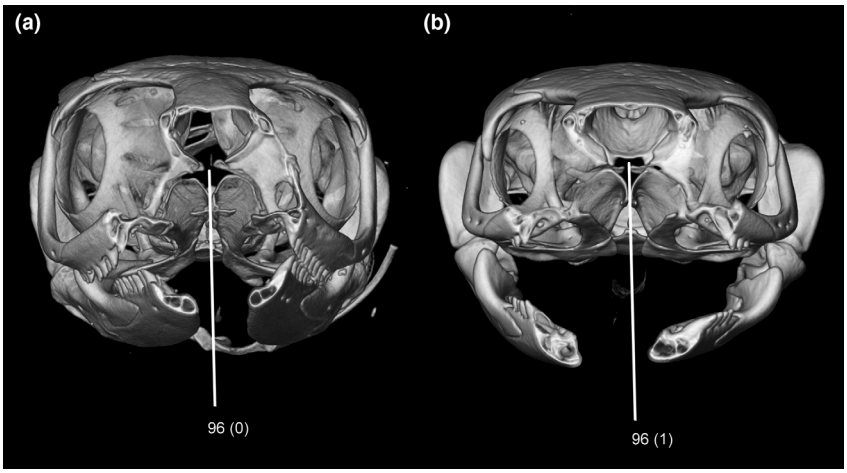

Fig. 14. The coronal plane cut of the skull of (a) *Loxopholis guianense* (HERR 15357), and (b) *Ptychoglossus vallensis* (AMNH 119239) showing the structure of the *cristae cranii*.

106. The prefrontal articulated with the palatine: (0) absent; (1) present.
107. Lacrimal bone in the adult forms: (0) absent; (1) present.
108. Postorbitofrontal: (0) absent; (1) present (MacLean, 1974; Presch, 1980; Fig. 16).
109. Postfrontal shape: (0) triradiated; (1) tetraradiated.

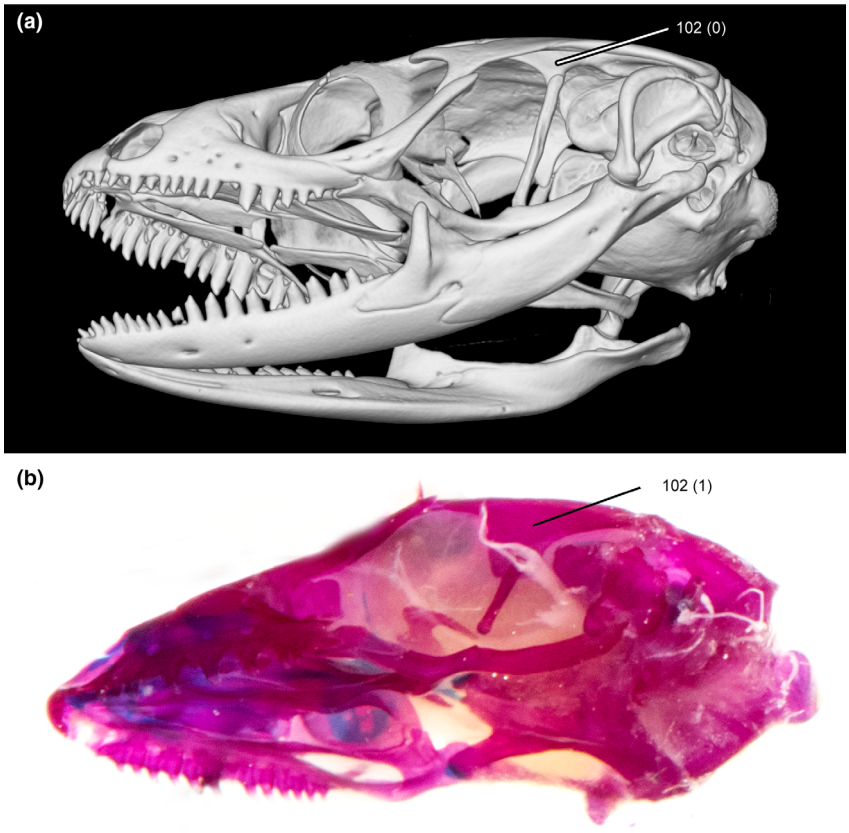

Fig. 15. Ventrolateral view of the skull in (a) *Ptychoglossus vallensis* (AMNH 119239), (b) *Bachia flavescens* (MPEG 27586). [Colour figure can be viewed at wileyonlinelibrary.com]

110. Jugal proportions: (0) dorsal process and suborbital process of the jugal with similar length; (1) suborbital process of the jugal conspicuously reduced.
111. Contact between the jugal and the postorbital or postorbitofrontal: (0) the tip of the dorsal process of the jugal articulates with the ventral tip of the ventral process of the postorbital (or postorbitofrontal); (1) the medial surface of the dorsal process of the jugal contacts the lateral surface of the ventral process of the postorbital (or postorbitofrontal); (2) the anterior border of the dorsal process of the jugal contacts the posterior border of the ventral process of the postorbital.
112. Proportion of dorsal and ventral rami of the pterygoid facet of the ectopterigoid: (0) dorsal and ventral rami with similar length; (1) without ventral rami.
113. Quadrate reduced: (0) absent; (1) present.
114. Dorsoanterior part of the tympanic crest of the quadrate: (0) convex, forming a continuous curved outline with the rest of the tympanic crest; (1) from flatter to slightly concave generating a discontinuity with the curved middle part of the tympanic crest.
115. Posterolateral process of the vomer: (0) absent; (1) present.
116. Contact between the palatine and the *cristae cranii* of the frontal: (0) absent; (1) present.
117. Palatines contact each another: (0) absent; (1) present.
118. Lateral border of the palatine with a shelf that projects medially: (0) absent; (1) present (Fig. 17).
119. Posteromedial process of the pterygoid (Hernandez-Morales et al., 2019): (0) present; (1) absent (Fig. 17).
120. Small conic tubercle protruding from the anterior border of the palatine process of the pterygoid: (0) absent; (1) present.
121. Pterygoid flange bifurcated: (0) absent; (1) present.
122. Basipterygoid process size: (0) small; (1) consciously projected (Fig. 17).
123. Basipterygoid process direction: (0) directed lateroventrally; (1) directed anteriorly.

Mandible ($n = 5$)

124. Meckel's groove: (0) open only anteriorly; (1) open from the middle to the anterior part of

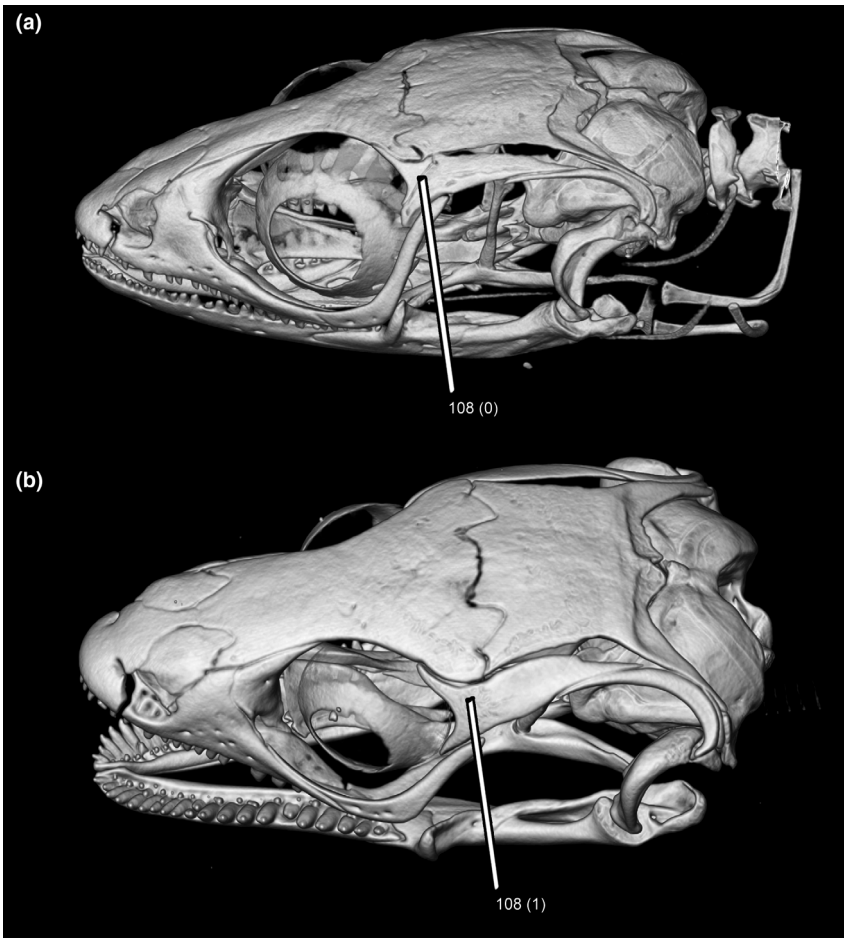

Fig. 16. Dorsolateral view of the skull in (a) *Cercosaura ocellata* (HERR 16695), and (b) *Ptychoglossus vallensis* (AMNH 119239).

the dentary; (2) encased in a tubular section of the dentary (MacLean, 1974; Presch, 1980).

125. Posterodorsal process of the dentary: (0) absent; (1) present.
126. Length of the anterior part of the splenial: (0) strongly projected anteriorly; (1) non or only slightly projected anteriorly.
127. Posterior process of the splenial: (0) truncated; (1) projected posteriorly.
128. Angular process of the mandible orientation: (0) ventromedially projected; (1) ventrally projected.

Hyoid apparatus (n = 5)

129. Hyoid cornu shape: (0) slender with parallel borders; (1) wide with rounded shape.
130. Lateral border of the hyoid cornu: (0) medially curved; (1) laterally curved.
131. Medial process of the hyoid cornu: (0) absent; (1) present.
132. Second ceratobranchial size: (0) goes posteriorly beyond the first ceratobranchial; (1) does not go beyond the first ceratobranchial; (2) absent.
133. First epibranchial with proximal expansion: (0) absent; (1) present.

Post-cranium (n = 10)

134. *Processus lingualis* with posterior expansion: (0) absent; (1) present.
135. Free epibranchial: (0) absent; (1) present.
136. Scapular fenestra: (0) absent; (1) present.
137. Interclavicle shape: (0) rod-shaped without lateral processes; (1) rhomboidally shaped with small lateral processes that go up the first coracoid fenestra; (2) cross-shaped with large lateral processes that can go beyond the second coracoid fenestra (Presch, 1980).
138. Phalanges of the first finger of the hand: (0) 2; (1) 1; (2) 0 (Roscito et al., 2014).
139. Size of fourth finger in relation to the third finger: (0) fourth finger longer than third finger;

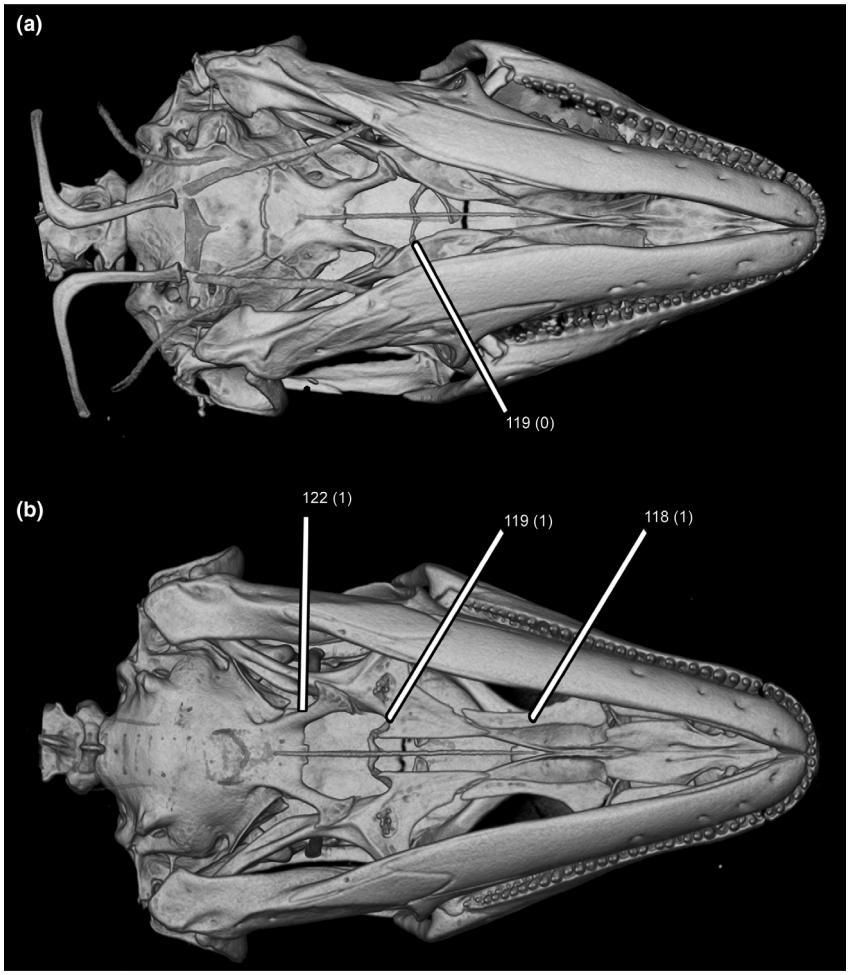

Fig. 17. Ventral view of the skull in (a) *Loxopholis guianense* (HERR 15357), and (b) *Alopoglossus buckleyi* (AMNH 113762).

(1) fourth finger shorter than or similar in length to third finger.

140. Ventral metacarpophalangeal sesamoids: (0) absent; (1) present.
141. Ventral distal phalangeal sesamoid: (0) absent; (1) present.
142. Dorsal distal phalangeal sesamoid: (0) absent; (1) present.
143. Position of the first caudal vertebrae with autotomy axis: (0) fifth vertebrae; (1) fourth vertebrae; (2) sixth vertebrae.